



**FÁTIMA MARIA PEREIRA DE REZENDE**

**PROBING SPIN-SPIN COUPLING CONSTANTS  
IN 2-HALOCYCLOHEXANONES AND  
2-HALOCYCLOHEXANOTHIONES: THE ROLE OF THE  
PERLIN, SOLVENT AND STEREOELECTRONIC EFFECTS**

**LAVRAS- MG  
2019**

**FÁTIMA MARIA PEREIRA DE REZENDE**

**PROBING SPIN-SPIN COUPLING CONSTANTS IN 2-HALOCYCLOHEXANONES  
AND 2-HALOCYCLOHEXANOTHIONES: THE ROLE OF THE PERLIN,  
SOLVENT AND STEREOELECTRONIC EFFECTS**

Tese apresentada à Universidade Federal de Lavras, como parte das exigências do Programa de Pós-Graduação em Agroquímica, área de concentração em Química/Bioquímica, para a obtenção do título de Doutora.

Prof. Dr. Teodorico de Castro Ramalho  
Orientador

Prof. Dr. Matheus Puggina de Freitas  
Coorientador

**LAVRAS – MG  
2019**

Ficha catalográfica elaborada pelo Sistema de Geração de Ficha Catalográfica da Biblioteca  
Universitária da UFLA, com dados informados pelo(a) próprio(a) autor(a).

Rezende, Fátima Maria Pereira de.

Probing spin-spin coupling constants in 2-halocyclohexanones  
and 2-halocyclohexanethiones: the role of the perlin, solvent and  
stereoelectronic effects. - 2019.

86 p. : il.

Orientador: Teodorico de Castro Ramalho.

Coorientador: Matheus Puggina de Freitas.

Tese (doutorado) - Universidade Federal de Lavras, 2019.

Bibliografia.

1. Long-range coupling. 2.  $^4J_{H_2,H_6}$ . 3. Perlin Effect. I. Ramalho,  
Teodorico de Castro. II. Freitas, Matheus Puggina de. III. Título.

**FÁTIMA MARIA PEREIRA DE REZENDE**

**PROBING SPIN-SPIN COUPLING CONSTANTS IN 2-HALOCYCLOHEXANONES  
AND 2-HALOCYCLOHEXANOTHIONES: THE ROLE OF THE PERLIN,  
SOLVENT AND STEREOELECTRONIC EFFECTS**

**SONDANDO A CONSTANTE DE ACOPLAMENTO SPIN-SPIN EM 2-  
HALOCICLOEXANONAS E 2-HALOCICLOTIOEXANONAS: O PAPEL DO  
EFEITO PERLIN, SOLVENTE E ESTEREOELETRÔNICO**

Tese apresentada à Universidade Federal de Lavras, como parte das exigências do Programa de Pós-Graduação em Agroquímica, área de concentração em Química/Bioquímica, para a obtenção do título de Doutora.

APROVADA em 18 de fevereiro de 2019.

Dr. Alison Geraldo Pacheco	IFSUL DE MINAS
Dra. Kátia Júlia de Almeida	UFLA
Dr. Luiz Antônio Sodré Costa	UFJF
Dr. Sérgio Sherrer Thomasi	UFLA

Prof. Dr. Teodorico de Castro Ramalho  
Orientador

Prof. Dr. Matheus Puggina de Freitas  
Coorientador

**LAVRAS–MG  
2019**

## AGRADECIMENTOS

Em primeiro lugar, gostaria de agradecer a Deus e a Nossa Senhora, por sempre me darem forças, bênçãos e por todas as graças recebidas.

À minha amada mãe Marisa pela paciência, conselhos, amor, zelo e apoio em todos os momentos da minha vida.

Ao meu amado pai Antônio (*in memoriam*), pelo imenso amor, ensinamentos, paciência, zelo e apoio. Pai saiba que mesmo ausente você sempre estará presente.

À minha amada irmã Franciely pelo amor, paciência, conselhos, zelo e pela alegria de todo o dia.

Ao meu orientador, Professor Teodorico, pela paciência, amizade, incentivo e apoio.

Ao meu coorientador, Professor Matheus, pela paciência, amizade e ensinamentos.

Aos membros da banca Professores: Alisson, Kátia, Luiz e Sérgio, pela disposição.

O presente trabalho foi realizado com apoio da Coordenação de Aperfeiçoamento de Pessoal de Nível Superior – Brasil (CAPES) – Código de Financiamento 001.

E ao CNPQ e a Fapemig.

## RESUMO

Estudos de acoplamento de longo alcance  ${}^4J_{H_2,H_6}$  foram realizados para 2-halo-cicloexanonas e ciclohexanotonas substituídas por (F, Cl e Br). Cálculos de NBO e constantes de acoplamento foram realizados com o objetivo de se avaliar o efeito do halogênio e do caráter aceptor de elétrons do orbital  $\pi^*$  sobre as referidas constantes de acoplamento. Os resultados apontaram interações hiperconjugativas  $\sigma_{C_2H_2} \rightarrow \pi^*_{C_1=Y}$  e  $\sigma_{C_6H_6} \rightarrow \pi^*_{C_1=Y}$  ( $Y = O$  e  $S$ ) para as formas equatoriais dos compostos substituídos por F, Cl e Br, as quais provavelmente contribuem para o mecanismo de transmissão de  ${}^4J_{H_2,H_6}$ . As interações  $\sigma_{C_2H_2} \rightarrow \pi^*_{C=Se}$  e  $\sigma_{C_6H_6} \rightarrow \pi^*_{C=S}$  são maiores para os compostos tiocarbonílicos, porém os valores de  ${}^4J_{H_2,H_6}$  são maiores para os compostos carbonílicos. Isso acontece porque o termo contato de Fermi (FC), que é influenciado pelo caráter s e comprimentos de ligação entre os átomos envolvidos na via de acoplamento, para os compostos tiocarbonílicos sofre um decaimento maior do que para as cetonas, reduzindo o valor de  ${}^4J_{H_2,H_6}$ . O efeito solvente implícito (DMSO e água) nos valores da constante de acoplamento foi insignificante quando comparado com a fase gasosa. Por outro lado, o efeito do solvente explícito em  ${}^4J_{H_2,H_6}$  foi mais sensível para os compostos tiocarbonílicos do que para as ciclohexanonas. Os diferentes halogênios não afetam a magnitude de  ${}^4J_{H_2,H_6}$ . Também foram efetuados estudos do efeito Perlin para 2-halo-cicloexanonas e ciclohexanotonas substituídas por (F, Cl e Br). O efeito Perlin é um fenômeno de RMN observado em anéis de seis membros e é referido como  ${}^1J_{C-H_{ax}} < {}^1J_{C-H_{eq}}$ . Neste presente trabalho, a influência de halogênios (F, Cl e Br) na posição 2 em ciclohexanonas e ciclohexanotonas é avaliada teoricamente nas constantes de acoplamento C2 – H2 de uma ligação, ou seja, no efeito Perlin. Uma interação hiperconjugativa importante ( $\pi_{C=Y} \rightarrow \sigma^*_{C-H}$ ,  $Y = O$  e  $S$ ) operando nos sistemas estudados parece desempenhar um papel significativo para o comportamento observado  ${}^1J_{C-H_{ax}} < {}^1J_{C-H_{eq}}$ . Além disso, a contribuição de Lewis ( $J^{Lewis}$ ) domina o termo de Contato Fermi ( $J^{FC}$ ), que desempenha o papel principal para a constante de acoplamento C-H de uma ligação geral. Em comparação com a fase gasosa, este comportamento foi considerado insensível a solventes implícitos (DMSO e água).

**Palavras-chave:** Acoplamento de longo alcance.  ${}^4J_{H_2,H_6}$ . Efeito Perlin. Hiperconjugação.

## ABSTRACT

Long-range coupling studies  ${}^4J_{\text{H}_2,\text{H}_6}$  were performed for 2-halo-cyclohexanones and cyclohexanones substituted by (F, Cl and Br). NBO calculations and coupling constants were performed with the objective of evaluating the effect of the halogen and electron acceptor character of the  $\pi^*$ orbital on the said coupling constants. The results pointed to hyperconjugative interactions  $\sigma_{\text{C}_2\text{H}_2} \rightarrow \pi^*_{\text{C}_1=\text{Y}}$  and  $\sigma_{\text{C}_6\text{H}_6} \rightarrow \pi^*_{\text{C}_1=\text{Y}}$  ( $\text{Y} = \text{O}$  and  $\text{S}$ ) for the equatorial forms of the compounds replaced by F, Cl and Br, which probably contribute to the mechanism of transmission of  ${}^4J_{\text{H}_2,\text{H}_6}$ . The interactions  $\sigma_{\text{C}_2\text{H}_2} \rightarrow \pi^*_{\text{C}_1=\text{Y}}$  and  $\sigma_{\text{C}_6\text{H}_6} \rightarrow \pi^*_{\text{C}_1=\text{Y}}$  are higher for thiocarbonyl compounds, but the values of  ${}^4J_{\text{H}_2,\text{H}_6}$  are higher for the carbonyl compounds. This is because the term Fermi (FC), which is influenced by the character of bonding lengths between the atoms involved in the coupling pathway, for thiocarbonyl compounds undergoes a larger decay than for the ketones, reducing the value of  ${}^4J_{\text{H}_2,\text{H}_6}$ . The implied solvent effect (DMSO and water) at the values of the coupling constant was insignificant when compared to the gas phase. On the other hand, the effect of the explicit solvent on  ${}^4J_{\text{H}_2,\text{H}_6}$  was more sensitive for thiocarbonyl compounds than for cyclohexanones. The different halogens do not affect the magnitude of  ${}^4J_{\text{H}_2,\text{H}_6}$ . Also performed were Perlin effect studies for 2-halo-cyclohexanones and cyclohexanones substituted by (F, Cl and Br). The Perlin effect is an NMR phenomenon observed in six-membered rings and is referred to as  ${}^1J_{\text{C-Hax}} < {}^1J_{\text{C-Heq}}$ . In this work, the influence of halogens (F, Cl and Br) at position 2 in cyclohexanones and cyclohexanones is theoretically evaluated in the C2 - H2 coupling constants of a bond, i.e. in the Perlin effect. An important hyperconjugative interaction ( $\pi_{\text{C}=\text{Y}} \rightarrow \sigma^*_{\text{C-H}}$ ,  $\text{Y} = \text{O}$  e  $\text{S}$ ) operating in the systems studied seems to play a significant role for the observed behavior of  ${}^1J_{\text{C-Hax}} < {}^1J_{\text{C-Heq}}$ . In addition, the contribution of Lewis ( ${}^1J_{\text{Lewis}}$ ) dominates the Fermi Contact term ( ${}^1J_{\text{FC}}$ ), which plays the leading role for the C-H coupling constant of a general bond. In comparison with the gas phase, this behavior was considered insensitive to implicit solvents (DMSO and water).

**Keywords:** Long-range coupling.  ${}^4J_{\text{H}_2,\text{H}_6}$ . Perlin Effect. Hyperconjugation.

## LISTA DE FIGURAS

### PRIMEIRA PARTE

Figura 1 –	2-Halo-cycloexanonas e 2-halo-cicloexanotionas teoricamente estudadas[1(Y = O, X = F); 2(Y = S, X = F); 3(Y = O, X = Cl); 4(Y = S, X = Cl); 5(Y = O, X = Br); 6(Y = S, X = Br)]. .....	15
Figura 2 –	Compostos com os respectivos valores de acoplamento para as formas axial e equatorial. ....	18
Figura 3 –	Compostos com os respectivos valores de acoplamento para as formas $\alpha$ e $\beta$ . ....	18
Figura 4 –	Isomerismo conformacional do metilcicloexano. ....	19
Figura 5 –	Interação hiperconjugativa $\sigma_{CH} \rightarrow \sigma^*_{C-H}$ no etano e estrutura de ressonância resultante dessa interação. ....	21

### SEGUNDA PARTE

#### ARTIGO 1

Figure 1 –	2-Halo-cyclohexanones and 2-halo-cyclohexanthonions theoretically studied (1: Y = O, X = F; 2: Y = S, X = F; 3: Y = O, X = Cl; 4: Y = S, X = Cl; 5: Y = O, X = Br; 6: Y = S, X = Br). ....	47
Figure 2 –	Resonance structure for the carbonyl (Y = O) and thiocarbonyl (Y = S) groups. Structure "b" contributes more for the resonance hybrid in the thiocarbonyl than in the carbonyl group. ....	48

#### ARTIGO 2

Figure 1 –	2-Halocyclohexanones [1 (X = F), 3(X = Cl) and 5 (X = Br), and Y = O] and 2- halocyclohexanthonions [2 (X = F), 4(X = Cl) and 6 (X = Br), and Y = S] theoretically studied.....	84
------------	---	----

## LISTA DE TABELAS

### SEGUNDA PARTE

#### ARTIGO1

Table 1 –	Calculated values for long-range coupling constants (Hz) for 2-halo-cyclohexanones and 2-halo-cyclohexanethiones. The data for the gas phase, DMSO, H <sub>2</sub> O (implicit solvent model-PCM) and explicit H <sub>2</sub> O are separated by bars. ....	41
Table 2 –	Hyperconjugative interactions (kcal mol <sup>-1</sup> ) relevant for 4JH <sub>2</sub> ,H <sub>6</sub> . Theoretical data (B3LYP/aug-cc-pVTZ) for the gas phase, DMSO, H <sub>2</sub> O (implicit solvent model-PCM) and H <sub>2</sub> O (explicit solvent) are separated by bars. ....	42
Table 3 –	FC, DSO, PSO and SD contributions for 4JH <sub>2</sub> ,H <sub>6</sub> (in Hz). ....	43
Table 4 –	% s character for the C1, C2 and C6 atoms in gas phase, DMSO, H <sub>2</sub> O (implicit solvent model-PCM) and H <sub>2</sub> O (explicit solvent) are separated by semicolons. ....	44
Table 5 –	Hyperconjugative interactions involving the $\pi_{C=Y}$ orbital (kcal mol <sup>-1</sup> ), gas phase, DMSO, H <sub>2</sub> O (implicit solvent model-PCM) and H <sub>2</sub> O (explicit solvent) are separated by semicolons and C-C and C-H (Å) bond distances, in the gas phase and explicit solvent (H <sub>2</sub> O) are separated by semicolons. ....	45
Table 6 –	NJC calculations (in Hz) for 4JH <sub>2</sub> ,H <sub>6</sub> . Theoretical data (B3LYP/aug-cc-pVTZ) for the gas phase. ....	46
Table S1 –	Calculated values for long-range coupling constants (Hz) for 2-halo-cyclohexanones and 2-halo-cyclohexanethiones. The data for the gas phase, DMSO, H <sub>2</sub> O (implicit solvent model-PCM) and explicit H <sub>2</sub> O are separated by stripes. ....	51
Table S2 –	Hyperconjugative interactions (kcal mol <sup>-1</sup> ) relevant for 4JH <sub>2</sub> ,H <sub>6</sub> . Theoretical data (B3LYP/aug-cc-pVTZ) for the gas phase, DMSO, H <sub>2</sub> O (implicit solvent model-PCM) and H <sub>2</sub> O (explicit solvent) are separated by stripes. ....	52
Table S3 –	X, Y and Z coordinates for 1ax in the gas. ....	53
Table S4 –	X, Y, Z coordinates for 1eq in the gas. ....	54
Table S5 –	X, Y and Z coordinates for 2ax in the gas. ....	55
Table S6 –	X, Y and Z coordinates for 2eq in the gas. ....	56
Table S7 –	X, Y and Z coordinates for 3ax in the gas. ....	57
Table S8 –	X, Y and Z coordinates for 3eq in the gas. ....	58

Table S9 –	X, Y and Z coordinates for 4ax in the gas. ....	59
Table S10 –	X, Y and Z coordinates for 4eq in the gas. ....	60
Table S11 –	X, Y and Z coordinates for 5ax in the gas. ....	61
Table S12 –	X, Y and Z coordinates for 5eq in the gas. ....	62
Table S13 –	X, Y and Z coordinates for 6ax in the gas. ....	63
Table S14 –	X, Y and Z coordinates for 6eq in the gas. ....	64

## ARTIGO 2

Table 1 –	Calculated relative conformational energies ( $E_{rel}$ in kcal mol <sup>-1</sup> , obtained at the $\omega$ B97X-D/6-31G(d,p) level), 1JC-H2 (in Hz, obtained at the $\omega$ B97X-D/6-311+G(d,p) level), molecular dipole moments ( $\mu$ , in Debye), and C–X bond lengths (in Å), for compounds 1-6.....	78
Table 2 –	NBO electron delocalization energies (in kcal mol <sup>-1</sup> ) obtained for 1-6 in the gas phase/DMSO/H2O.....	79
Table 3 –	The Ramsey terms (Fermi contact, spin dipolar, paramagnetic spin-orbit, and diamagnetic spin-orbit) for 1JC-H (in Hz) in 1-6 (gas phase/DMSO/water). ....	80
Table 4 –	% s-character for the C2, Hax and Heq atoms in gas phase/DMSO/H2O).....	81
Table 5 –	Electronic occupancies at $\sigma$ C–H2 in gas phase/DMSO/H2O. ....	82
Table 6 –	NJC results (in Hz) for 1JC-H. Theoretical data obtained at the $\omega$ B97XD/6-31g (d,p) level for the gas phase molecules. ....	83

## LISTA DE ABREVIATURAS

Ax	Axial
Eq	Equatorial
SSCC	Constante de acoplamiento spin-spin
THP	Tetrahidropirano

## LISTA DE SIGLAS

ADF	<i>Application Development Framework</i>
deloc	Deslocalização
DFT	Teoria do Funcional de Densidade
DMC	Dinâmica Molecular Clássica
DMQ	Dinâmica Molecular Quântica
DSO	Diamagnético spin-órbita
FC	Contato de Fermi
NBO	Orbitais Naturais de Ligação
NJC	Análise de acoplamentos $J$ naturais
NMR	Ressonância Magnética Nuclear
Occ	Ocupado
PCM	Modelo Contínuo Polarizável
PSO	Paramagnético spin-órbita
QIP	<i>Quantum Information Processing</i>
repol	Repolarização
SD	Diamagnético spin-órbita
Unocc	Desocupado

## LISTA DE SÍMBOLOS

Å	Ångström
Hz	Hertz
kcalmol <sup>-1</sup>	Quilocaloria por mol

## SUMÁRIO

1	<b>INTRODUÇÃO GERAL.....</b>	<b>14</b>
2	<b>REFERENCIAL TEÓRICO.....</b>	<b>17</b>
2.1	<b>Efeito Perlin.....</b>	<b>17</b>
2.2	<b>Efeito do solvente.....</b>	<b>18</b>
2.3	<b>Efeitos estereoeletrônicos.....</b>	<b>19</b>
2.4	<b>Breve descrição dos modelos de cálculos teóricos.....</b>	<b>21</b>
2.5	<b>Dinâmica molecular e dinâmica quântica.....</b>	<b>22</b>
2.6	<b>Ressonância magnética nuclear.....</b>	<b>23</b>
2.7	<b>Análise de acoplamento de <i>J</i>-naturais.....</b>	<b>24</b>
2.8	<b>Caráter <i>s</i>.....</b>	<b>25</b>
	<b>REFERÊNCIAS.....</b>	<b>26</b>
	<b>SEGUNDA PARTE – ARTIGOS.....</b>	<b>31</b>
	<b>ARTIGO 1 – Probing long-range spin-spin coupling constants in 2-halo-substituted cyclohexanones and cyclohexanethiones: the role of solvent and stereoelectronic effects.....</b>	<b>31</b>
	<b>ARTIGO 2 – The Perlin effect in 2-halocyclohexanones and 2-halocyclohexanethiones.....</b>	<b>65</b>
3	<b>CONCLUSÃO GERAL.....</b>	<b>85</b>

## PRIMEIRA PARTE

### 1 INTRODUÇÃO GERAL

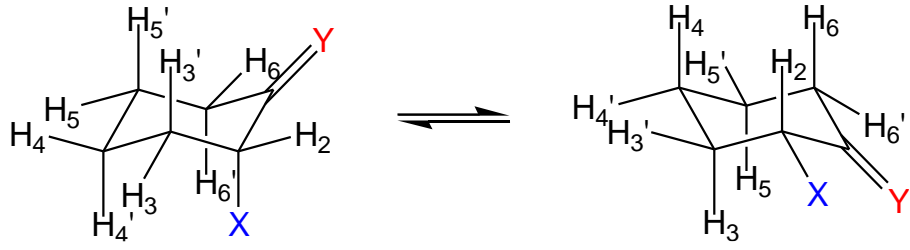
O acoplamento spin-spin é a interação nuclear entre o spin nuclear de um átomo com o spin nuclear de outro átomo por meio das ligações químicas. É bem conhecida a constante de acoplamento na química orgânica, uma vez que auxilia na elucidação de estruturas (SILVERSTEIN; WEBSTER, 2000). São quatro as contribuições que descrevem o valor teórico da constante de acoplamento indireta spin-spin: o termo diamagnético spin órbita (DSO), o paramagnético spin órbita (PSO), o spin dipolar (SD) e o termo de contato de Fermi (FC) (DOS SANTOS, 2009; HELGAKER; JASZUŃSKI; PECUL, 2008). Embora na maioria dos casos o termo FC descreva quase que totalmente o valor da constante de acoplamento envolvendo núcleos de  $^1\text{H}$  e  $^{13}\text{C}$ , as outras contribuições não podem, *a priori*, serem negligenciadas, o que aumenta a necessidade de maiores esforços computacionais. Em segundo lugar, os termos FC e SD envolvem perturbações em estado excitado tripleto, o que requer uma descrição flexível da estrutura eletrônica molecular. E, finalmente, para que um cálculo descreva com precisão o termo FC, é necessário descrever com precisão a densidade eletrônica próxima do núcleo atômico (elétrons nos orbitais s). Por estes motivos, o cálculo de constante de acoplamento para sistemas moleculares grandes apresenta-se com uma dificuldade para a química computacional (DOS SANTOS, 2009; HELGAKER; MICHAŁ; RUUD, 1999; RAMSEY, 1953).

O termo de contato de Fermi surge devido à polarização de spin do sistema eletrônico causado por um núcleo, que resulta de uma interação de transferência desta polarização de spin para outro núcleo. Teoricamente o núcleo é tratado como pontos de carga e dipolos magnéticos, o termo “contato”, surge principalmente devido à interação local do núcleo com o spin local dos elétrons, que seriam, portanto, os pontos de carga. O restante da interação entre o spin nuclear com o spin eletrônico é um dipolo magnético que é descrito pelo operador spin-dipolar (SD). O mecanismo orbital eletrônico é dividido em uma contribuição paramagnética (PSO) e diamagnética (DSO). Teoricamente eles podem ser distinguidos como dois operadores independentes, entretanto apenas sua soma apresenta significado físico. O mecanismo PSO, tipicamente, apresenta valores pequenos, enquanto o mecanismo DSO é usualmente negligenciado. É interessante ressaltar que experimentalmente o acoplamento J é soma de todos estes mecanismos. E o acoplamento J é positivo ou negativo dependendo da influência relativa de cada mecanismo e das razões magnetogíricas de cada núcleo (DOS SANTOS, 2009).

Nesse contexto, compostos carbonílicos são de grande relevância na Química Orgânica, uma vez que o grupo C=O possui forte reatividade e tem como característica singular o forte caráter doador e aceptor de elétrons (COELHO; FREITAS; RAMALHO, 2008; RAUK, 2001). Estudos já realizados para as formas axial e equatorial da 2-bromocicloexanona, tendo como intuito avaliar o acoplamento de longo alcance  $^4J_{H_2,H_6}$  e sua origem no confôrmero equatorial, apontaram que o mecanismo de transmissão da constante de acoplamento  $^4J_{H_2,H_6}$  envolve interações hiperconjugativas:  $\sigma_{C_2H_2} \rightarrow \pi^*_{C_1=O}$  e  $\sigma_{C_6H_6} \rightarrow \pi^*_{C_1=O}$  (COELHO et al., 2009). Apesar de grande importância, ainda há pouca investigação sobre o grupo tiocarbonila (C=S), e os relatos existentes são limitados a descrever os níveis de orbitais e sua aplicação em síntese e à grande reatividade desse grupo (ALLENMARK et al., 1984; COELHO; FREITAS; RAMALHO, 2008).

Com este propósito, objetivou-se avaliar o acoplamento de longo alcance  $^4J_{H_2,H_6}$  e seu mecanismo de transmissão nas formas axial e equatorial da 2-halocicloexanona e 2-halocicloexanotona, sendo X = F, Cl e Br. Com também, avaliar o efeito Perlin do solvente e a interferência dos halogênios nas moléculas de 2-halocicloexanona e 2-halocicloexanotona, sendo X= F, Cl e Br. Para tanto, no primeiro artigo será avaliado os mecanismos de transmissão da constante de acoplamento  $^4J_{H_2,H_6}$  em cicloexanonas e cicloexanotonas 2-halossustituídas (halo = F, Cl e Br) e, por conseguinte, obter informação a respeito da relação entre interações hiperconjugativas e os grupos substituintes e carbonila/tiocarbonila. Os compostos descritos na Figura 1 serão estudados teoricamente neste primeiro artigo. No segundo artigo, será avaliado a influência de halogênios (F, Cl e Br) na posição 2 em cicloexanonas e cicloexanotonas nas constantes de acoplamento  $^1J_{C_2-H_2}$  de uma ligação, ou seja, a interferência de (F, Cl e Br) no efeito Perlin que refere-se ao menor valor da constante de acoplamento spin-spin  $^1J_{C-H_{axial}}$  em comparação com o correspondente  $^1J_{C-H_{eq}}$  em anel de seis membros. Os compostos que serão estudados neste segundo artigo estão representados na Figura 1 (SILLA et al., 2014).

Figura 1 – 2-Halo-cycloexanonas e 2-halo-cicloexanotonas teoricamente estudadas [1(Y = O, X = F); 2(Y = S, X = F); 3(Y = O, X = Cl); 4(Y = S, X = Cl); 5(Y = O, X = Br); 6(Y = S, X = Br)].



## 2 REFERENCIAL TEÓRICO

### 2.1 Efeito Perlin

O efeito Perlin se refere ao menor valor de constante de acoplamento spin-spin  $^1J_{C-H_{ax}}$  em comparação com o valor correspondente de  $^1J_{C-H_{eq}}$  em anéis de 6 membros. Originalmente, esse fenômeno foi atribuído ao fato de que as ligações C – H<sub>ax</sub> são mais longas que C – H<sub>eq</sub>, devido à deslocalização eletrônica preferencial envolvendo orbitais antiperiplanares portadores de H<sub>ax</sub> em vez de H<sub>eq</sub>. Isso ocorre devido, a interação  $\pi_{CO} \rightarrow \sigma^*_{CF}$  em derivados de cicloexano, como na Figura 2, e a interação  $n_O \rightarrow \sigma^*_{C-H_{ax}}$  em derivados de tetraidropirano, como açúcares piranosídicos. O efeito Perlin reverso corresponde a  $^1J_{C-H_{ax}}$  constante de acoplamento spin-spin maior que  $^1J_{C-H_{eq}}$  em alguns ditianos, devido a melhor transferência de elétrons  $\sigma_{CS} \rightarrow \sigma^*_{C-H_{eq}}$  do que  $n_S \rightarrow \sigma^*_{C-H_{ax}}$  (JURIASTI, 2012; SILLA et al., 2014), foram observados o efeito Perlin reverso nas constante de acoplamento  $^1J_{C-F}$  do composto tetracetato de 2-fluór- $\alpha$ - $\beta$ -glucopiranosil, Figura 3 (SILLA et al., 2014).

Por causa da interpretação baseada na hiperconjugação, o efeito Perlin tem sido frequentemente relacionado ao efeito anomérico, que é um conceito em química de carboidratos e pode ser definido como a preferência de substituintes eletronegativos (X) ligados ao carbono anomérico para ocupar uma orientação axial. ( $\alpha$ -anômero) em vez da orientação equatorial menos impedida ( $\beta$ -anômero) que seria esperada em considerações estéricas de uma conformação de cadeira (ELIEL, 1972; SILLA et al., 2014).

A relação entre os dois efeitos provém do fato de que a ligação C<sub>2</sub>-H<sub>ax</sub> é maior em relação à ligação C<sub>2</sub>-H<sub>eq</sub> em tetraidropirano (THP), que seria a consequência da origem hiperconjugativa do efeito anomérico (a interação  $n_O \rightarrow \sigma^*_{C-H_{ax}}$  em THP ou  $n_O \rightarrow \sigma^*_{CX}$  em 2-X-THP) (ALABUGIN, 2000; SILLA et al., 2014) e a causa de o efeito Perlin ( $^1J_{C-H_{ax}} < ^1J_{C-H_{eq}}$ , já que as ligações C – H mais longas dificultam a transmissão do acoplamento). Vale ressaltar que os efeitos estruturais nas ligações C - H não associadas à hiperconjugação foram relatados em heterociclos de seis membros (ALABUGIN; MANOHARAN; ZEIDAN, 2003; SILLA et al., 2014). Além disso, os efeitos eletrostáticos também são operativos e foram invocados para explicar ambos os efeitos (MO, 2010; SILLA et al., 2014).

Figura 2 – Compostos com os respectivos valores de acoplamento para as formas axial e equatorial.

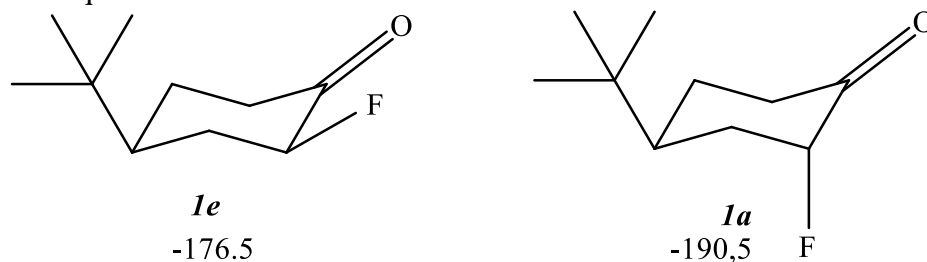
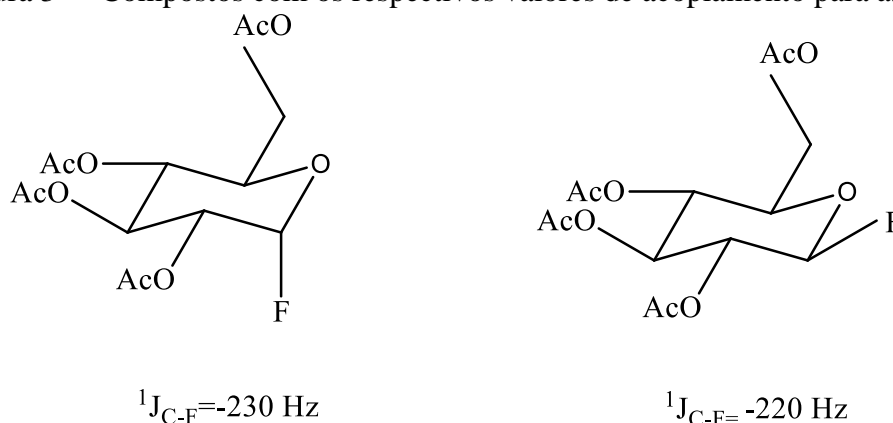


Figura 3 – Compostos com os respectivos valores de acoplamento para as formas  $\alpha$  e  $\beta$ .



## 2.2 Efeito do solvente

Muitos equilíbrios químicos são modificados por uma mudança no ambiente químico por isso o efeito do solvente desempenha um papel especial na química orgânica. O efeito do solvente no equilíbrio conformacional é particularmente importante quando os confôrmeros em equilíbrio têm diferentes momentos de dipolo, e é frequentemente racionalizado em termos da interação intermolecular eletrostática soluto-solvente (YARDAKUL; TANRIBUYU, 2013). Problemas relativos aos fenômenos que ocorrem em solução e a influência do solvente no comportamento estrutural das moléculas de soluto são de interesse para a química, bioquímica e física (BUISSONNEAUD; MOURIK; O'HAGAN, 2010; CRAMER; TRUHLAR, 1999; YARDAKUL; TANRIBUYU, 2013).

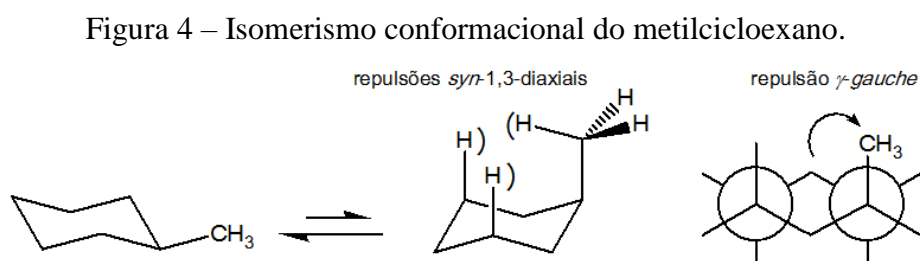
O efeito do solvente é considerado fundamental para o desenho de fármacos na indústria farmacêutica, pois esse efeito afeta a liberação, transporte e degradação da droga no organismo (TIWARY; MISHRA, 2009; YARDAKUL; TANRIBUYU, 2013). Efeitos do solvente são usualmente tratados teoricamente em dois segmentos. O efeito do solvente explícito consiste em incluir um determinado número de moléculas de solvente ao redor de moléculas de soluto.

Já no efeito do solvente implícito, a molécula de soluto é introduzida em uma cavidade cercada por um meio de constante dielétrica ( $\epsilon$ ), correspondente à do solvente que se deseja analisar (YARDAKUL; TANRIBUYU, 2013).

O modelo PCM foi integrado com êxito nos estudos que evidenciam os efeitos de moléculas de soluto no solvente. Segundo esse modelo, o efeito de polarização é calculado por integração numérica e a cavidade do soluto é definida como um conjunto de esferas unidas, em que cada uma delas representa um átomo em particular (FORESMAN; FRISCH, 1996; TOMASI; MENNUCCI; CAMMI, 2005; SILLA, 2013). Constantes de acoplamento indireta spin-spin foram estudadas em um protótipo contra a doença de chagas, para a avaliação de J envolvendo o átomo de N com o par de elétrons solitários, a molécula foi estudada em diferentes meios: gás, solvente água de modo implícito (modelo PCM) e afim de se avaliar ligações de hidrogênio foram usadas moléculas de água explícita, uma vez que o modelo PCM não descreve realisticamente tais interações intermoleculares (RAMALHO; PEREIRA; THIEL, 2011).

### 2.3 Efeitos estereoeletrônicos

O efeito estérico é uma função de tamanho e orientação de grupos, e pode ser avaliado, por exemplo, comparando-se o volume atômico do hidrogênio (um grupo substituinte padrão com o menor volume atômico) com o volume de outros grupos substituintes. O efeito estérico também é usado para justificar a estabilidade conformacional de moléculas; por exemplo, a conformação preferencial do metilcicloexano é a *equatorial*, em razão da repulsão estérica envolvendo o grupo metila *axial*, Figura 4 (FREITAS; RAMALHO, 2013).



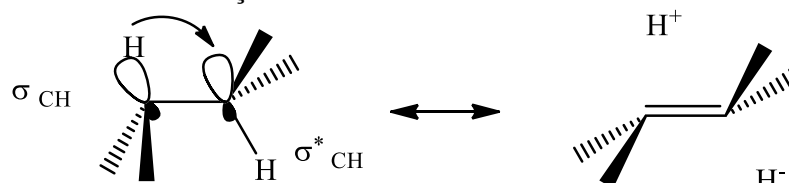
Interações estabilizantes entre orbitais em moléculas podem ser exibidos através da hiperconjugação (ALABUGIN; GILMORE; PETERSON, 2011). Esse efeito descreve as consequências da deslocalização eletrônica e pode ser expressa como a diferença entre uma estrutura perfeitamente localizada, a de Lewis, e uma molécula real. Embora a interação de

orbitais- $\pi$ , ou conjugação, tenha sido uma característica teórica proeminente na química orgânica por um longo período de tempo, a importância da deslocalização de interações que envolvam ligações  $\sigma$  (ALABUGIN; GILMORE; PETERSON, 2011; DEWAR, 1962; REED; CURTISS; WEINHOLD, 1988) não foi igualmente reconhecida, embora Mulliken tenha publicado trabalhos pioneiros em 1940 sobre a hiperconjugação (ALABUGIN; GILMORE; PETERSON, 2011; MULLIKEN, 1939; MULLIKEN; RIEKE; BROWN, 1941). Esta situação tem mudado não somente porque as ligações- $\sigma$  são muito mais comuns do que as ligações- $\pi$  e, assim, as interações hiperconjugativas têm apresentado aplicabilidades na química, mas principalmente devido ao acúmulo do significativo valor teórico e experimental e evidências de que estas interações levam a uma significativa mudança na geometria, densidade de elétrons, energia de orbitais moleculares, espectros no infravermelho, ligações de pontos fortes (efeito Bohhmann) (ALABUGIN; GILMORE; PETERSON, 2011; BOHLMANN, 1957; WOLFE; KIM, 1991) e propriedades de ressonância magnética nuclear (ALABUGIN; GILMORE; PETERSON, 2011; JUARISTI; CUEVAS, 2007).

Em muitos casos a hiperconjugação influencia em equilíbrios conformacionais (ALABUGIN; GILMORE; PETERSON, 2011; CRAMER; 1996; GOODMAN; GU; POPHRISTIC, 1999; GRACZYK; MIKOLAJCZYK, 1994; JUARISTI; CUEVAS, 1992; LU; WEINHOLD; WEISHAAR, 1995; POPHRISTIC; GOODMAN; GUCHHAIT, 1997; REED; WEINHOLD, 1991; ROMERS et al., 1969; UEHARA et al., 1999; ZEFIROV; SCHECHTMAN, 1971), modifica a reatividade (ALABUGIN; GILMORE; PETERSON, 2011; BADDELEY, 1973; BORDEN, 1998; CHANG et al., 1987; DESLONGCHAMPS, 1975; LAMBERT et al., 1999; MAIER, 2000; ROBERTS; STEEL, 1993; UM; CHUNG; LEE, 1998; WAGNER; SCHEVE, 1977) e determina a seletividade (BECHWITH; DUGGAN, 1998). A hiperconjugação é definida como interações do tipo  $\sigma \rightarrow \pi^*$ ,  $\pi \rightarrow \sigma^*$  e  $\sigma \rightarrow \sigma^*$ . Dado que os efeitos acima mencionados descrevem o mesmo fenômeno fundamental e são diferentes apenas dentro do modelo  $\sigma$ - $\pi$ , a sua separação tem um valor, sobretudo histórico. Para a interação estar se estabilizando, o orbital de maior energia tem de ser parcialmente vazio (zero ou um elétron), e o de menor energia tem de estar pelo menos parcialmente cheio. O cenário mais comum, corresponde a um dos dois elétrons da interação, onde o orbital de menor energia (uma ligação ou par solitário) que está completamente cheio passa para o orbital antiligante vazio (ALABUGIN; GILMORE; PETERSON, 2011). A hiperconjugação é comumente expressa como uma contribuição de ressonância, indicando que os elétrons das ligações não são localizados (Figura 5); assim como para o benzeno, guardadas as devidas proporções, a ressonância no etano também é estabilizante. A interpretação de que interações

hiperconjugativas dominam a estabilidade de forma alternada do etano também é estabilizante. A interpretação de que as interações hiperconjugativas dominam a estabilidade da forma alternada do etano tem sido contestada na literatura (BICKELHAUPT; BAERENDS, 2003; FREITAS; RAMALHO, 2013; MO, GAO, 2007).

Figura 5 – Interação hiperconjugativa  $\sigma_{CH} \rightarrow \sigma^*_{C-H}$  no etano e estrutura de ressonância resultante dessa interação.



A influência da interação hiperconjugativa, por exemplo do tipo  $n \rightarrow \sigma^*$ , no acoplamento  $^1J_{CH}$  tem sido amplamente estudada por vários autores (BADENHOOP; WEINHOLD, 1997; CUEVAS; JUARISTI; VELA, 1999; JUARISTI; CUEVAS; VELA, 1994; MARTÍNEZ-MAYORGA; JUARISTI; CUEVAS, 2004; SANTOS et al., 2007). Estudos realizados por Cuevas, Juaristi e Vela (1999), com 1,3-ditianos e 1,3-dioxanos mostraram que as constantes de acoplamento  $^1J_{CH}$  são muito sensíveis às orientações entre os pares de elétrons dos átomos de enxofre e oxigênio e à ligação C-H, pois são observados dois valores para o acoplamento  $^1J_{CH}$ , um para o H na orientação axial e outro para o H na equatorial.

## 2.4 Breve descrição dos modelos de cálculos teóricos

Os métodos da estrutura eletrônica empregam as leis da mecânica quântica ao invés das leis da física clássica como base para seus cálculos. Os métodos da estrutura eletrônica podem ser semi-empíricos ou *ab initio*. Os métodos semi-empíricos usam parâmetros derivados de dados experimentais para simplificar os cálculos. Por outro lado, os métodos *ab initio* não utilizam nenhum parâmetro experimental, apenas os valores de poucas constantes físicas: velocidade da luz, massa e carga do elétron e dos núcleos e a constante de Planck (FORESMAN; FRISCH, 1996; MARTINS, 2009). No caso de moléculas simples, os cálculos *ab initio* são os que têm sido mais utilizados e fornecem informações a respeito das diferenças de energia entre os confôrmeros mais estáveis, os momentos de dipolo e as geometrias de cada possível confôrmero no vácuo (FRISCH et al., 2009; MARTINS, 2009).

Dentre os métodos *ab initio*, o método Hartree-Fock (HF) produz um modelo razoável para um grande número de sistemas moleculares. Porém, a teoria Hartree-Fock tem suas

limitações; elas surgem principalmente do fato que esta teoria não inclui um tratamento dos efeitos da correlação eletrônica, ou seja, não levam em consideração as interações entre os elétrons, pois os elétrons, em um sistema molecular, interagem entre si e tendem a se permanecer afastados (MARTINS, 2009). Para suprir esta limitação, um grande número de métodos foi desenvolvido, os quais incluem alguns efeitos de correlação eletrônica. Dentre eles, podemos destacar o método MP2 (teoria de perturbação de segunda ordem Möller Plesset) (MØLLER; PLESSET, 1934), o qual contabiliza as interações instantâneas dos pares de elétrons com spins opostos (FORESMAN; FRISCH, 1996; MARTINS, 2009).

Portanto, cálculos com teoria MP2 ou outros métodos que levam em consideração as correlações eletrônicas fornecem resultados mais precisos, principalmente em se tratando da geometria molecular e energias, pois há uma diferença considerável nas geometrias obtidas para uma determinada molécula quando se faz uso da teoria HF e quando se utiliza a teoria MP2. Porém, a teoria MP2 necessita de recursos computacionais mais sofisticados, pois seu cálculo é mais complexo. Atualmente, uma terceira classe de métodos da estrutura eletrônica, os métodos da teoria do funcional de densidade (DFT) têm sido amplamente empregados. Estes métodos são similares aos métodos *ab initio* em muitos aspectos. O método DFT alcança melhor precisão do que a teoria HF com somente um modesto aumento de custo (tempo de processamento), porém menor do que o MP2. Os métodos DFT também incluem alguns dos efeitos de correlação eletrônica muito menos dispendiosos do que os métodos de correlação tradicionais (MARTINS, 2009).

## 2.5 Dinâmica molecular e dinâmica quântica

A simulação de dinâmica molecular clássica (DM) é uma das técnicas mais versáteis para o estudo de macromoléculas. No planejamento científico (físico-químico) de novas estruturas, as simulações de DM são fundamentais em diversos estágios do processo. A metodologia da Dinâmica Molecular Clássica (DMC) é fundamentada nos princípios de Mecânica Clássica e fornece informações sobre o comportamento dinâmico microscópico, dependente do tempo, dos átomos individuais que compõe o sistema. Para se obter as propriedades de interesse, é necessário aplicar a mecânica estatística, a qual tem função de calcular propriedades interessantes na química como: temperatura, pressão, volume, energia interna, entropia, etc. A DMC é calculada definindo um campo de força pelo qual é possível calcular as forças que atuam sobre cada átomo, calculando-se a primeira derivada da energia potencial, obtida do campo de força escolhido, em relação às posições desses átomos (NAMBA;

DA SILVA; DA SILVA, 2008). Já a simulação de dinâmica molecular quântica (DMQ) envolve a convergência da função de onda do sistema para cada passo da simulação. A DMQ apresenta vantagens significativas para estudos que envolvem estruturas e propriedades eletrônicas de sistemas moleculares complexos. Porém, uma das suas desvantagens é o elevado custo computacional, quando comparado aos métodos de dinâmica molecular clássicos (MANCINI, 2014).

## 2.6 Ressonância magnética nuclear

A espectrometria de ressonância magnética nuclear (RMN) é basicamente uma outra forma de espectroscopia de absorção, semelhante à espectrometria de infravermelho e à de ultravioleta. Sob condições apropriadas em um campo magnético, uma amostra pode absorver radiação eletromagnética na região de radiofrequências (rf) em uma frequência regida pelas características estruturais da amostra. A absorção é função de determinados núcleos da molécula. Um espectro de RMN é um registro gráfico das frequências dos picos de absorção contra suas intensidades. (SILVERSTEIN; WEBSTER, 2000).

O núcleo de  $^{12}\text{C}$  não é magneticamente “ativo”(o número de spin,  $I$ , é igual a zero). O núcleo de  $^{13}\text{C}$ , porém, tem, como, o núcleo  $^1\text{H}$ , número de spin igual a  $1/2$ . Como entretanto, a abundância natural de  $^{13}\text{C}$  é só 1,1% da de  $^{12}\text{C}$  e sua sensibilidade apenas 1,6% da de  $^1\text{H}$ , a sensibilidade total do núcleo de  $^{13}\text{C}$ , em comparação com  $^1\text{H}$ , é de cerca de  $1/5.700$ . Os núcleos de  $^{13}\text{C}$  distribuem-se em uma faixa mais ampla em comparação com os hidrogênios. Os núcleos de  $^{13}\text{C}$  são muito menos abundantes e muito menos sensíveis do que os hidrogênios. Amostras maiores e maiores tempos de irradiação são necessários (SILVERSTEIN; WEBSTER, 2000).

Depois do carbono e hidrogênio, os núcleos mais importantes em compostos orgânicos são o oxigênio e o nitrogênio. Para o químico orgânico, a presença de um desses elementos na molécula significa a existência de “grupos funcionais”.  $^{17}\text{O}$  tem spin  $5/2$  e não é muito utilizado em estudos de RMN, e  $^{16}\text{O}$  tem spin zero. O nitrogênio, por outro lado, tem dois isótopos magneticamente ativos,  $^{14}\text{N}$  e  $^{15}\text{N}$ . Ambos os isótopos têm sido alvo de estudos intensivos de RMN. O RMN de  $^{19}\text{F}$  tem enorme importância histórica. O flúor tem apenas isótopo natural, o  $^{19}\text{F}$ . A sensibilidade de  $^{19}\text{F}$  é igual a cerca de 0,82 vez a sensibilidade de  $^1\text{H}$ , e isso permitiu que o desenvolvimento da RMN de  $^{19}\text{F}$  ocorresse paralelamente ao da RMN de  $^1\text{H}$ . Já o silício, como o flúor, não ocorre naturalmente nos compostos orgânicos. Os compostos orgânicos que contêm silício, entretanto, estão sendo cada vez mais usados pelos químicos orgânicos de

síntese. O núcleo  $^{29}\text{Si}$  tem abundância natural de 4,7% e é o único isótopo do silício com momento magnético diferente de zero. E, por fim,  $^{31}\text{P}$  é único isótopo natural do fósforo, nuclídeo tem spin  $\frac{1}{2}$  e razão magnetogírica positiva (10.840) (SILVERSTEIN; WEBSTER, 2000).

## 2.7 Análise de acoplamento de $J$ -naturais

A análise de acoplamento  $J$ -natural (NJC) analisa a porção de contato Fermi do acoplamento  $J$ . A abordagem baseia-se nos conceitos e formalismos dos métodos orbitais de ligação natural (NBO). Contribuições de acoplamento computadorizados podem ser classificadas como Lewis (contribuições orbitais individuais correspondentes à estrutura natural de Lewis da molécula), deslocalização (resultante de interações doadoras/aceitadoras emparelhadas) e repolarização residual (correspondendo a interações semelhantes à correlação). O termo FC pode ser completamente avaliado através de cálculos de NJC, outro aspecto interessante a considerar em relação ao termo FC é a contribuição de Lewis e de não-Lewis para por exemplo o  $^1J^{\text{FC}}_{\text{C-H}_2}$ , que foi decomposto nessas contribuições (Equação 2) (WILKENS et al., 2001), com base em uma análise NJC.

$$\Delta^1 J^{\text{FC}}_{\text{C-H}_2} = \Delta^1 J^{\text{Lewis}}_{\text{C-H}_2} + \Delta^1 J^{\text{non-Lewis}}_{\text{C-H}_2} \quad (2)$$

A contribuição de Lewis reflete o caráter do orbital de acordo com um esquema baseado em Lewis (isto é, considerando a ligação, par solitário ou orbital central), enquanto a parte não-Lewis está relacionada a todos os efeitos de deslocalização não descritos no esquema de Lewis. Em outras palavras, Lewis ou contribuições localizadas correspondem a interações estéricas, enquanto as interações não-Lewis são aquelas derivadas de deslocalizações de densidade de elétrons. Dentro do NBO-NJC, o termo não-Lewis é dividido em duas contribuições: aquelas que correspondem à transferência da densidade eletrônica de um orbital doador para um aceitador centrado em uma região diferente da molécula, a chamada parte deslocalizada. Além disso, há também transferência em torno do orbital centralizado na mesma região de conexão, chamada de contribuição de repolarização, de acordo com a Equação 3 (WILKENS et al., 2001).

$$\Delta^1 J^{\text{non-Lewis}}_{\text{C-H}_2} = \Delta^1 J^{\text{deloc}}_{\text{C-H}_2} + \Delta^1 J^{\text{repol}}_{\text{C-H}_2} \quad (3)$$

Além disso,  $\Delta^1 J_{\text{C2-H2}}^{\text{Lewis}}$  e  $\Delta^1 J_{\text{C2-H2}}^{\text{non-Lewis}}$  podem ser decomposto em contribuições individuais de diferentes NBOs, ocupados e desocupados, de acordo com as Equações 4 e 5 (WILKENS et al., 2001).

$$\Delta^1 J_{\text{HH}}^{\text{Lewis}} = \sum_i^{\text{Occ}} \Delta_i^{\text{Lewis}} \quad (4)$$

$$\Delta^1 J_{\text{HH}}^{\text{non-Lewis}} = \sum_i^{\text{Occ}} \sum_i^{\text{Unocc}} \Delta_{ij}^{\text{non-Lewis}} \quad (5)$$

## 2.8 Caráter *s*

O comprimento das ligações é diferente em função do tipo de ligação. Os orbitais *s*, também chamados de orbitais de caroço, estão mais próximos do núcleo atômico do que um orbital *p*, o que permite que sua interação com o núcleo seja consideravelmente maior quando comparado à interação entre o núcleo e os orbitais *p*. Sendo assim, quanto maior o caráter *s* do orbital híbrido, menor o comprimento da ligação, tendo em vista a proximidade entre o orbital *s* e o núcleo. Assim, em ligações triplas, onde o átomo de carbono apresenta hibridização *sp* (formado por porcentagens equivalentes de orbitais *s* e *p*) são mais curtas que as ligações duplas (*sp*<sup>2</sup>: 33,3% +66,7% *p*), que por sua vez, são mais curtas que as ligações simples (25% de *s* +75% de *p*). Quanto maior o caráter *s* de um orbital hibridizado, mais eletronegativo ele será. Desta forma, um orbital *sp* é mais eletronegativo do que *sp*<sup>2</sup> e este mais eletronegativo do que um orbital *sp*<sup>3</sup> (SANTOS et al., 2007). Assim para o estudo do caráter *s*, é importante mencionar que o termo FC é influenciado pela hibridização dos carbonos que participam do caminho do acoplamento (sendo que um menor caráter *s* induz a um decaimento no valor de *J*), bem como pelo comprimento das ligações C-C e C-H envolvidas no caminho do acoplamento (RUSAKOV; KRIVDIN,2013).

## REFERÊNCIAS

- ALABUGIN, I. V. Stereoelectronic interactions in cyclohexane, 1, 3-dioxane, 1, 3-oxathiane, and 1, 3-dithiane: W-effect,  $\sigma\text{C-X} \leftrightarrow \sigma^* \text{CH}$  interactions, anomeric effect what is really important?. **The Journal of Organic Chemistry**, Washington, v. 65, n. 13, p. 3910-3919, 2000.
- ALABUGIN, I. V.; GILMORE, K. M.; PETERSON, P. W. Hyperconjugation. **WIREs Computational Molecular Science**, Hoboken, v. 1, n. 1, p. 109-141, 2011.
- ALABUGIN, I. V.; MANOHARAN, M.; ZEIDAN, T. A. Homoanomeric effects in six-membered heterocycles. **Journal of the American Chemical Society**, Washington, v. 125, n. 46, p. 14014-14031, 2003.
- ALLENMARK, S. et al. Direct optical resolution of a series of pharmacologically active racemic sulfoxides by high-performance liquid affinity chromatography. **Analytical Biochemistry**, San Diego, v. 136, n. 2, p. 293-297, 1984.
- BADDELEY, G. Delocalization into anti antibond orbitals. **Tetrahedron Letters**, Oxford, v. 14, n. 18, p. 1645-1648, 1973.
- BADENHOOP, J. K.; WEINHOLD, F. Natural bond orbital analysis of steric interactions. **The Journal of Chemical Physics**, Melville, v. 107, n. 14, p. 5406-5421, 1997.
- BECKWITH, A. L. J.; DUGGAN, P. J. The quasi-homo-anomeric interaction in substituted tetrahydropyranyl radicals: diastereoselectivity. **Tetrahedron**, Oxford, v. 54, n. 24, p. 6919-6928, 1998.
- BICHELHAUPT, F. M.; BAERENDS, E. J. The case for steric repulsion causing the staggered conformation of ethane. **Angewandte Chemie International Edition**, Weinheim, v. 42, n. 35, p. 4183-4188, 2003.
- BOHLMANN, F. Configuration determination of quinolizidine derivatives. **Angewandte Chemie**, Weinheim, v. 69, p. 641-642, 1957.
- BORDEN, W. T. Effects of electron donation into C F  $\sigma^*$ -orbitals: explanations, predictions and experimental tests. **Chemical Communications**, Cambridge, v. 18, n. 18, p. 1919-1925, 1998.
- BUISSONNEAUD, D. Y.; MOURIK, T. V.; O'HAGAN, D. A DFT study on the origin of the fluorine gauche effect. **Tetrahedron**, Oxford, v. 66, n. 12, p. 2196-2202, 2010.
- CHANG, J. W. A. et al. Stereoelectronic effects on the nucleophilic addition of phosphate to the carbonyl double bond: Ab initio molecular orbital calculations on reaction surfaces and the  $\sigma$ -effect. **Tetrahedron**, Oxford, v. 43, n. 17, p. 3863-3874, 1987.
- COELHO, J. V.; FREITAS, M. P.; RAMALHO, T. C. The role of carbonyl and thiocarbonyl groups in the conformational isomerism of haloacetones and halothioacetones. **Structural Chemistry**, New York, v. 19, n. 4, p. 671-677, 2008.

COELHO, J. V. et al. On the  $^4J_{H,H}$  long-range coupling in 2-bromocyclohexanone: conformational insights. **Magnetic Resonance in Chemistry**, Hoboken, v. 47, n. 4, p. 348-351, 2009.

CRAMER, C. J.; TRUHLAR, D. G. Implicit solvation models: equilibria, structure, spectra, and dynamics. **Chemical Reviews**, Washington, v. 99, n. 8, p. 2161-2200, 1999.

CRAMER, C. J. Hyperconjugation as it effects conformational analysis. **Journal of Molecular Structure**, Amsterdam, v. 370, n. 2-3, p. 135-146, 1996.

CUEVAS, G.; JUARISTI, E.; VELA, A. Density functional calculation of  $^1J_{CH}$  coupling constants in cyclohexane and diheterocyclohexanes: Repercussion of stereoelectronic effects on coupling constants. **The Journal of Physical Chemistry A**, Washington, v. 103, n. 7, p. 932-937, 1999.

DESLONGCHAMPS, P. Stereoelectronic control in the cleavage of tetrahedral intermediates in the hydrolysis of esters and amides. **Tetrahedron**, Oxford, v. 31, n. 20, p. 2463-2490, 1975.

DEWAR, M. J. S. **Hyperconjugation**. New York: Ronald Press Co., 1962.

DOS SANTOS, F. P. **Determinação e análise das constantes de acoplamento  $^nJ_{CH}$  (n= 2, 3, 4) em derivados do norbornano**. 2009. 134 p. Tese (Doutorado em Química Orgânica) - Universidade Estadual de Campinas, Campinas, 2009.

ELIEL, E. L. Conformational analysis in heterocyclic systems: recent results and applications. **Angewandte Chemie**, Weinheim, v. 11, n. 9, p. 739-750, 1972.

FREITAS, M. P.; RAMALHO, T. C. **Princípios de estrutura eletrônica e orbitais em química orgânica**. Lavras: UFLA, 2013. 126 p.

FRISCH, M. J. et al. **Gaussian 09: Revision D.01**. Wallingford: Gaussian Inc., 2009.

FORESMAN, J. B.; FRISCH, A. E. **Exploring chemistry with electronic structure methods**. 2. ed. Pittsburg: Gaussian, 1996. 302 p.

GOODMAN, L.; GU, H.; POPHRISTIC, V. Flexing analysis of ethane internal rotation energetics. **The Journal of Chemical Physics**, Melville, v. 110, n. 9, p. 4268-4275, 1999.

GRACZYK, P. P.; MIKOLAJCZYK, M. Anomeric effect: origin and consequences. **Topics in Stereochemistry**, Hoboken, v. 21, p. 159-349, 1994.

HELGAKER, T.; MICHAŁ, J.; RUUD, K. Ab initio methods for the calculation of NMR shielding and indirect spin-spin coupling constants. **Chemical Reviews**, Washington, v. 99, n. 1, p. 293-352, 1999.

HELGAKER, T.; JASZUŃSKI, M.; PECUL, M. The quantum-chemical calculation of NMR indirect spin-spin coupling constants. **Progress in Nuclear Magnetic Resonance Spectroscopy**, Oxford, v. 53, n. 4, p. 249-268, 2008.

JUARISTI, E. Looking for treasure in stereochemistry-land: A path marked by curiosity, obstinacy, and serendipity. **The Journal of Organic Chemistry**, Washington, v. 77, n. 11, p. 4861-4884, 2012.

JUARISTI, E.; CUEVAS, G. Manifestations of stereoelectronic interactions in 1JC-Hone-bond coupling constants. **Accounts of Chemical Research**, Washington, v. 40, n. 10, p. 961-970, 2007.

JUARISTI, E.; CUEVAS, G. Recent studies on the anomeric effect. **Tetrahedron**, Oxford, v. 48, n. 24, p. 5019-5087, 1992.

JUARISTI, E.; CUEVAS, G.; VELA, A. Stereoelectronic interpretation for the anomalous <sup>1</sup>H NMR chemical shifts and one-bond CH coupling constants (Perlin effects) in 1, 3-dioxanes, 1, 3-oxathianes, and 1, 3-dithianes: Spectroscopic and theoretical observations. **Journal of the American Chemical Society**, Washington, v. 116, n. 13, p. 5796-5804, 1994.

LAMBERT, J. B. et al. The  $\beta$ -effect of silicon and related manifestations of  $\sigma$ conjugation. **Accounts of Chemical Research**, Washington, v. 32, n. 2, p. 183-190, 1999.

LU, K. T.; WEINHOLD, F.; WEISHAAR, J. C. Understanding barriers to internal rotation in substituted toluenes and their cations. **The Journal of Chemical Physics**, Melville, v. 102, n. 17, p. 6787-6805, 1995.

MAIER, M. E. Synthesis of medium-sized rings by thering-closing metathesis reaction. **Angewandte Chemie**, Weinheim, v. 39, n. 12, p. 2073-2077, 2000.

MANCINI, D. T. **Fenilbenzotiazóis como sonda espectroscópica para biomoléculas: cálculo de propriedades estruturais e eletrônicas**. 2014. 157 p. Tese (Doutorado em Agroquímica) - Universidade Federal de Lavras, Lavras, 2014.

MARTÍNEZ-MAYORGA, K.; JUARISTI, E.; CUEVAS, G. Manifestation of stereoelectronic effects on the calculated carbon-hydrogen bond lengths and one-bond <sup>1</sup>J CH NMR coupling constants: Relative acceptor ability of the carbonyl (CO), thiocarbonyl (CS), and methylenic (C=CH<sub>2</sub>) groups toward C-H donor bonds. **The Journal of Organic Chemistry**, Washington, v. 69, n. 21, p. 7266-7276, 2004.

MARTINS, C. R. **Estudos conformacional de ésteres metálicos de alguns aminoácidos através das espectroscopias no infravermelho, de RMN e cálculos teóricos**. 2009. 101 p. Tese (Doutorado em Química Orgânica) - Universidade Estadual de Campinas, Campinas, 2009.

MØLLER, C.; PLESSET, M. S. Note on an approximation treatment for many-electron systems. **Physical Review**, College Park, v. 46, n. 7, p. 618-622, 1934.

MO, Y. Computational evidence that hyperconjugative interactions are not responsible for the anomeric effect. **Nature Chemistry**, London, v. 2, n. 8, p. 666-671, 2010.

MO, Y.; GAO, J. Theoretical analysis of the rotational barrier of ethane. **Accounts of Chemical Research**, Washington, v. 40, n. 2, p. 113-119, 2007.

MULLIKEN, R. S. Intensities of electronic transitions in molecular spectra. IV: Cyclic dienes and hyperconjugation. **The Journal of Chemical Physics**, Melville, v. 7, n. 5, p. 339-352, 1939.

MULLIKEN, R. S.; RIEKE, C. A., BROWN, W. G. Hyperconjugation. **Journal of the American Chemical Society**, Washington, v. 63, n. 1, p. 41-56, 1941.

NAMBA, A. M.; DA SILVA, V. B.; DA SILVA, C. H. T. P. Dinâmica molecular: teoria e aplicações em planejamento de fármacos. **Eclética Química**, São Paulo, v. 33, n. 4, p. 13-23, 2008.

POPHRISTIC, V.; GOODMAN, L., GUCHHAIT, N. Role of lone-pairs in internal rotation barriers. **The Journal of Physical Chemistry A**, Washington, v. 101, n. 23, p. 4290-4297, 1997.

RAMALHO, T. C.; PEREIRA, D. H.; THIEL, W. Thermal and solvent effects on NMR indirect spin-spin coupling constants of a prototypical Chagas disease drug. **The Journal of Physical Chemistry A**, Washington, v. 115, n. 46, p. 13504-13512, 2011.

RAMSEY, N. F. Electron coupled interactions between nuclear spins in molecules. **Physical Review**, College Park, v. 91, n. 2, p. 303-307, 1953.

RAUK, A. **Orbital interaction theory of organic chemistry**. 2. ed. New York: J. Wiley, 2001. 360 p.

REED, A. E.; CURTISS, L. A.; WEINHOLD, F. Intermolecular interactions from a natural bond orbital, donor-acceptor viewpoint. **Chemical Reviews**, Washington, v. 88, n. 6, p. 899-926, 1988.

REED, A. E.; WEINHOLD, F. Natural bond orbital analysis of internal rotation barriers and related phenomena. **Israel Journal of Chemistry**, Weinheim, v. 31, n. 4, p. 277-285, 1991.

ROBERTS, B. P.; STEEL, A. J. The substituent effect of a  $\beta$ -carbon-oxygen bond in radical reactions. **Tetrahedron Letters**, Oxford, v. 34, n. 32, p. 5167-5170, 1993.

ROMERS, C. et al. Geometry and conformational properties of some five- and six-membered heterocyclic compounds containing oxygen or sulfur. **Topics in Stereochemistry**, Hoboken, v. 4, p. 39-97, 1969.

RUSAKOV, Y. Y.; KRIVDIN, L. B. Modern quantum chemical methods for calculating spin-spin coupling constants: theoretical basis and structural applications in chemistry. **Russian Chemical Reviews**, Bristol, v. 82, n. 2, p. 99-130, 2013.

SANTOS, F. P. et al. Efeito das interações hiperconjugativas na constante de acoplamento  $^1J_{CH}$  da hexametilenotetramina e do adamantano: estudo teórico e experimental. **Química Nova**, São Paulo, v. 30, n. 7, p. 1681-1685, 2007.

SILLA, J. M. **Análise conformacional e interações intramoleculares em ácidos aromáticos fluorados e derivados**. 2013. 121 p. Dissertação (Mestrado em Agroquímica) - Universidade Federal de Lavras, Lavras, 2013.

SILLA, J. M. et al. The reverse fluorine perlin-like effect and related stereoelectronic interactions. **The Journal of Organic Chemistry**, Washington, v. 79, n. 13, p. 6385-6388, 2014.

SILVERSTEIN, R. M.; WEBSTER, F. X. **Identificação espectrométrica de compostos orgânicos**. 6. ed. Rio de Janeiro: LTC, 2000. 460 p.

TIWARY, S.; MISHRA, P. C. Vibrational spectra of cysteine zwitterion and mechanism of its formation: bulk and specific solvent effects and geometry optimization in aqueous media. **Spectrochimica Acta Part A - Molecular and Biomolecular Spectroscopy**, Oxford, v. 73, n. 4, p. 719-729, 2009.

TOMASI, J.; MENNUCCI, B.; CAMMI, R. Quantum mechanical continuum solvation models. **Chemical Reviews**, Washington, v. 105, n. 8, p. 2999-3093, 2005.

UEHARA, F. et al. The effect of a para substituent on the conformational preference of 2,2-diphenyl-1,3-dioxanes: evidence for the anomeric effect from X-ray crystal structure analysis. **The Journal of Organic Chemistry**, Washington, v. 64, n. 5, p. 1436-1441, 1999.

UM, I. H.; CHUNG, E. K.; LEE, S. M. An unusual ground-state stabilization effect and origins of the  $\sigma$ -effect in aminolyses of Y-substituted phenyl X-substituted benzoates. **Canadian Journal of Chemistry**, Ottawa, v. 76, n. 6, p. 729-737, 1998.

WAGNER, P. J.; SCHEVE, B. J. Absence of intramolecular charge-transfer quenching in photoexcited 4-benzoylpiperidines. **Journal of the American Chemical Society**, Washington, v. 99, n. 6, p. 1858-1863, 1977.

WILKENS, S. J. et al. Natural J-coupling analysis: Interpretation of scalar J-couplings in terms of natural bond orbitals. **Journal of the American Chemical Society**, Washington, v. 123, n. 48, p. 12026-12036, 2001.

WOLFE, S.; KIM, C. K. A theoretical study of conformational deuterium isotope effects and bond dissociation energies of diastereotopic hydrogens. **Canadian Journal of Chemistry**, Ottawa, v. 69, n. 9, p. 1408-1412, 1991.

YARDAKUL, S.; TANRIBUYU, S. Theoretical and experimental study of solvent effects on the structure, vibrational spectra, and tautomerism of 3-amino-1,2,4-triazine. **Journal of Molecular Structure**, Amsterdam, v. 1052, p. 57-66, 2013.

ZEFIROV, N. S.; SCHECHTMAN, N. M. Anomeric effect. **Uspekhi Khimii**, Moscow, v. 40, p. 593-624, 1971.

**SEGUNDA PARTE – ARTIGOS****ARTIGO 1****Probing long-range spin-spin coupling constants in 2-halo-substituted cyclohexanones and cyclohexanethiones: the role of solvent and stereoelectronic effects**

Fátima M. P. de Rezende<sup>1</sup>, Matheus P. Freitas<sup>1</sup>, Teodorico C. Ramalho<sup>1,2\*</sup>

<sup>1</sup>Department of Chemistry, Federal University of Lavras, 37200-000, Lavras, MG, Brazil.

<sup>2</sup>Center for Basic and Applied Research, Faculty of Informatics and Management, University of Hradec Kralove, Rokitanskeho 62, 50003, Czech Republic.

\*Corresponding author

E-mail: teo@dqi.ufla.br

Phone: (+55) (35) 3829-1522

**Study coupling of  $^4J$  to cyclohexanones and cyclohexanethiones**

**Normas do Periódico: Magnetic Resonance in Chemistry  
(versão publicada)**

## ABSTRACT

Earlier studies with 2-bromocyclohexanone demonstrated a measurable long-range coupling constant ( ${}^4J_{\text{H2,H6}}$ ) for the equatorial conformer, while  ${}^4J_{\text{H2,H4}}$  and  ${}^4J_{\text{H4,H6}}$  were not observed; as a consequence, it is inferred that the carbonyl group plays an important role particularly due to hyperconjugative interactions  $\sigma_{\text{C2H2}} \rightarrow \pi^*_{\text{C=O}}$  and  $\sigma_{\text{C6H6}} \rightarrow \pi^*_{\text{C=O}}$ . In the present study, NBO analysis and coupling constant calculations were performed to cyclohexanone and cyclohexanethione alpha substituted with F, Cl and Br, aiming to evaluate the halogen effect and acceptor character of the  $\pi^*$  orbital on the long-range coupling pathway. The  $\sigma_{\text{C2H2}} \rightarrow \pi^*_{\text{C1=Y}}$  and  $\sigma_{\text{C6H6}} \rightarrow \pi^*_{\text{C1=Y}}$  ( $\text{Y} = \text{O}$  e  $\text{S}$ ) hyperconjugative interactions for the equatorial conformer indeed contribute for the  ${}^4J_{\text{H2,H6}}$  transmission mechanism. Surprisingly, the  ${}^4J_{\text{H2,H6}}$  value is higher for the carbonyl compounds, although the interactions  $\sigma_{\text{C2H2}} \rightarrow \pi^*_{\text{C=Y}}$  and  $\sigma_{\text{C6H6}} \rightarrow \pi^*_{\text{C=Y}}$  are more efficient for the thiocarbonyl compounds. Accordingly, the Fermi Contact (FC) contribution for the thiocarbonyl compounds decays deeper than in ketones, thus reducing more the  ${}^4J_{\text{H2,H6}}$  values. Moreover, both  $\pi_{\text{C=S}} \rightarrow \sigma^*_{\text{C-X}}$  and  $\pi_{\text{C=S}} \rightarrow \sigma^*_{\text{C-H}}$  interactions seem to be stronger in thiocarbonyl than in carbonylic compounds. The implicit solvent effect (DMSO and water) on the coupling constant values was negligible when compared to the gas phase. On the other hand, an explicit solvent effect was found and  ${}^4J_{\text{H2,H6}}$  for the thiocarbonyl compounds appeared to be more sensitive than for the cyclohexanones.

## KEYWORDS

${}^4J_{\text{H2,H6}}$ , long-range, stereoelectronic effects, halogen, Fermi contact

## 1 INTRODUCTION

Carbonyl compounds are of great relevance in Organic Chemistry, since the C=O group is highly reactive and has as singular characteristic owing to its strongly electron donor and acceptor character.<sup>[1,2]</sup> Some studies have shown that hyperconjugation plays an important role in the stabilization of conformers containing the C=O group.<sup>[2-5]</sup> The axial and equatorial preferences for the substituent at position 2 in cyclohexanones has been attributed to classical interactions, solvent effects and electron delocalization from a substituent lone pair and the neighboring empty orbital  $\pi^*_{\text{C=O}}$ .<sup>[2-8]</sup>

It has been shown that 2-bromocyclohexanone experiences a long-range coupling constant  $^4J_{\text{H}_2,\text{H}_6}$  in both the axial and equatorial conformers, whose transmission mechanism in the equatorial conformer has been pointed out to be dependent on hyperconjugative interactions:  $\sigma_{\text{C}_2\text{H}_2} \rightarrow \pi^*_{\text{C}_1=\text{O}}$  and  $\sigma_{\text{C}_6\text{H}_6} \rightarrow \pi^*_{\text{C}_1=\text{O}}$ .<sup>[9]</sup> This spectroscopic result is, in fact, an experimental evidence that hyperconjugative interactions contribute to the conformational stabilization of 2-bromocyclohexanone as well as are strongly related to NMR parameters of 2-halo-substituted cyclohexanones and cyclohexanethiones.

Recently, NMR techniques are the most widely used for the structural characterization of the widest array of molecules, complexes and molecular aggregates.<sup>[10]</sup> It should be kept in mind, however, that it is difficult to confirm or establish assignments of NMR signals as well as provide a basis for interpretation of their positions in the spectrum and their fine structure. In this line, theoretical calculations based on density functional theory can provide a reliable framework to predict spectroscopic parameters (chemical shifts and coupling constants, generally involving  $^1\text{H}$  and  $^{13}\text{C}$ ) of organic or inorganic compounds with useful accuracy.<sup>[10-12]</sup>

Despite the importance of this topic in *e.g.* spectroscopy and organic synthesis, there are only few NMR studies focused on the thiocarbonyl group (C=S), and the current efforts are most interested in describing the orbital levels and their application in synthesis and the great reactivity of this group.<sup>[2-9, 13]</sup> Thus, theoretical studies have been performed in order to evaluate the transmission mechanisms of the  $^4J_{\text{H}_2,\text{H}_6}$  coupling constant in 2-halosubstituted cyclohexanones and cyclohexanethiones (halo = F, Cl and Br) and, therefore, information regarding the effects of hyperconjugative interactions and substituents in compounds **1-6** of Figure 1 on  $^4J_{\text{H}_2,\text{H}_6}$  can be provided. Spin-spin couplings in a molecule are also essential for the implementation of Quantum Information Processing (QIP).<sup>[14]</sup>

## 2 COMPUTATIONAL METHODS

Geometry optimization for the compounds of Figure 1 was performed at the MP2/aug-cc-pVTZ<sup>[15-18]</sup> level using the Gaussian 09 program.<sup>[19]</sup> Hyperconjugative interactions were evaluated by natural bond orbital (NBO)<sup>[19]</sup> at the B3LYP-aug-cc-pVTZ level.<sup>[16-18, 20, 21]</sup> In addition, natural J-coupling analysis was performed through the NJC method<sup>[22]</sup> implemented within the NBO at the B3LYP-aug-cc-pVTZ level.<sup>[16-18, 20, 21]</sup> DFT calculations with the B3LYP functional were also used to determine the coupling constants  $^3J_{H_2,H_3}$ ,  $^3J_{H_2,H_4}$ ,  $^4J_{H_4,H_6}$  and  $^4J_{H_2,H_6}$ . The EPR-III basis set was employed for the H and F atoms and, for C, S, O, Br, Cl, the aug-cc-pVTZ basis set was used. All calculations were performed for the gas phase and using an implicit solution scheme (Polarizable Continuous Model - PCM<sup>[23]</sup>) for DMSO and H<sub>2</sub>O.

An explicit solvation (water) environment was applied over the optimized structures, using molecular dynamics simulations with the ADF program<sup>[24]</sup> (reax extension), considering 400000 interactions and 300 water molecules. After the classical molecular dynamics, the last conformation was selected and quantum dynamics calculations were performed using the Gaussian09 program, at 298 K., because it is not a compound with biological activity. Additionally, with the aim of exploring the relativistic effects, including scalar and spin-orbit, for the compounds with bromine, relativistic DFT calculations were employed using the ADF software.<sup>[24-25]</sup>

## 3 RESULTS AND DISCUSSION

NMR calculations for all compounds with bromine atoms (**5a**, **5e**, **6a** and **6e**) were carried out with and without the inclusion of relativistic effects. From our findings, a little difference was observed in the coupling constant values without and with scalar relativistic effects as well as spin-orbit coupling relativistic effects. For **5a**, ( $\Delta J=|0.001|$  Hz and  $|0.015|$  Hz for scalar and spin-orbit relativistic effects, respectively); **5e** ( $\Delta J=|0.006|$  and  $|0.035|$  Hz for scalar and spin-orbit relativistic effects, respectively), **6a** ( $\Delta J=|0.028|$  and  $|0.028|$  Hz for scalar and spin-orbit relativistic effects, respectively) and **6e** ( $\Delta J=|0.045|$  and  $|0.025|$  Hz for scalar and spin-orbit relativistic effect, respectively). Thus, in the current work, the relativistic effects are not considered, whereas previous findings indicate that relativistic effects on the NMR properties can be significant with the presence of bromine atoms in organic molecules.<sup>[26]</sup>

The antiperiplanar orientation for the H<sub>2</sub>-C-C-H<sub>3</sub> dihedral angle in the equatorial conformer ( $\approx 180^\circ$ ) is expected to yield higher values for  $^3J_{H_2,H_3}$  when compared to the axial

conformer ( $\text{H}_2\text{-C-C-H}_3 \approx 60^\circ$ ), as formerly described by Karplus<sup>[27-29]</sup> (Table 1). However, four-bond coupling constants is small or even unobserved in conformationally flexible compounds. Indeed, the calculated  $^4J_{\text{H}_2,\text{H}_4}$  and  $^4J_{\text{H}_4,\text{H}_6}$  long-range coupling constants were calculated to be near zero, but the calculated  $^4J_{\text{H}_2,\text{H}_6}$  coupling constants for **1-6** were within 1-2 Hz (Table 1). This is reproduced experimentally for 2-bromocyclohexanone<sup>[9]</sup>, whose  $^4J_{\text{H}_2,\text{H}_6}$  is *ca.* 1.5 Hz and the carbonyl group was indicated as the key pathway for the transmission of this coupling, by means of relevant hyperconjugative interactions  $\sigma_{\text{C}_2\text{-H}_2} \rightarrow \pi^*_{\text{C=O}}$  and  $\sigma_{\text{C}_6\text{H}_6} \rightarrow \pi^*_{\text{C=O}}$ .

For the cyclohexanones **1**, **3** and **5**, there is not strong dependence of  $\sigma_{\text{C}_2\text{-H}_2} \rightarrow \pi^*_{\text{C=O}}$  and  $\sigma_{\text{C}_6\text{H}_6} \rightarrow \pi^*_{\text{C=O}}$  interactions with the halogen, neither of other electron delocalizations affecting the occupancy of antibonding orbitals involved in the  $^4J_{\text{H}_2,\text{H}_6}$  coupling pathway, namely  $n_{\text{O}} \rightarrow \sigma^*_{\text{C}_1\text{-C}_2}$  and  $n_{\text{O}} \rightarrow \sigma^*_{\text{C}_1\text{-C}_6}$  (Table 2). In addition, solvent changes do not affect these interactions significantly. This behavior is consistent with the fact that, for the carbonyl compounds,  $^4J_{\text{H}_2,\text{H}_6}$  is insensitive to halogen. For instance, consider the series C-X (X = F, Cl, Br and I), where the most labile bond is C-I. It is worth noting that the fragility of the C-I bond can determine the great tendency of the  $\sigma^*_{\text{C}_1\text{-I}}$  orbital to receive electron<sup>[30-31]</sup> as well as to influence spectroscopic properties more significantly than other halo-substituted compounds.<sup>[31]</sup> This is experimentally corroborated by the rigid derivatives *cis* and *trans*-4-*t*-butyl-2-bromocyclohexanone, whose  $^4J_{\text{H}_2,\text{H}_6}$  values are 0.9 and 1.2 Hz, respectively, either in  $\text{CCl}_4$  or  $\text{CD}_3\text{CN}$  solution.<sup>[32]</sup> It is important to keep in mind that some hyperconjugative interactions are not indicated in Tables 2 and 5, because they are smaller than the threshold value.

The electronic interactions for the thiocarbonyl compounds **2eq**, **4eq** and **6eq** are stronger than for the corresponding carbonyl compounds **1eq**, **3eq** and **5eq** (Table 2), because of the strongest electron donor character of  $n_{\text{S}}$  and better electron acceptor ability of the  $\sigma^*_{\text{C}_1\text{-C}_2}$  and  $\pi^*_{\text{C=S}}$  orbitals. Surprisingly, smaller  $^4J_{\text{H}_2,\text{H}_6}$  values were obtained for the thiocarbonyl compounds (*ca.* 2 Hz for the carbonyl and 1 Hz for the thiocarbonyl compounds), despite their more efficient hyperconjugative interactions. This apparent contradiction is supported by the Fermi (FC) contact term reported in Table 3, which can be used to rationalize the  $^4J_{\text{H}_2,\text{H}_6}$  values. The other contribution from spin-dipolar (SD), paramagnetic spin-orbit (PSO) and diamagnetic (DSO) do not vary significantly between carbonyl and thiocarbonyl compounds. It is worth mentioning that the FC term is influenced by the hybridization of the carbons that are participating in the coupling pathway (a lower *s* character - Table 4 - induces a decay in the *J* value), as well as the bond lengths C-C and C-H involved in the coupling pathway.<sup>[33]</sup> Interactions  $\pi_{\text{C=Y}} \rightarrow \sigma^*_{\text{C}_X}$  and  $\pi_{\text{C=Y}} \rightarrow \sigma^*_{\text{C}_H}$ , which are more effective in the thiocarbonyl

compounds, affect the C1, C2 and C6 hybridizations, as well as the bond lengths C-C and C-H (Table 5). Thus, the difference of *ca.* 1 Hz in  ${}^4J_{\text{H}_2,\text{H}_6}$  between carbonyl and thiocarbonyl compounds is mirrored by the FC term.

In an explicit solvent model, which accounts for specific solute-solvent interactions (such as hydrogen bonding), the  ${}^3J_{\text{H}_2,\text{H}_3}$  values of Table 1 are of course larger for the equatorial conformers, as predicted by the Karplus relationship.<sup>[27-29]</sup> Similarly to that obtained in the gas phase and implicit solvents, the long-range coupling constants  ${}^4J$  are small and possibly undetectable in explicit water solvent, unless the  ${}^4J_{\text{H}_2,\text{H}_6}$ . For cyclohexanones **1eq**, **3eq** and **5eq**, this coupling constant is about 2 Hz (Table 1), in agreement with the values obtained for the gas phase and implicit solvent, where differences of only *ca.* 0.2-0.3 Hz were found. Thus,  ${}^4J_{\text{H}_2,\text{H}_6}$  appears to be insensitive to the halogen and solvent, as the above-mentioned interactions  $\sigma_{\text{C}_2\text{-H}_2} \rightarrow \pi^*_{\text{C}=\text{O}}$ ,  $\sigma_{\text{C}_6\text{H}_6} \rightarrow \pi^*_{\text{C}=\text{O}}$ ,  $n_{\text{O}} \rightarrow \sigma^*_{\text{C}_1\text{-C}_2}$  and  $n_{\text{O}} \rightarrow \sigma^*_{\text{C}_1\text{-C}_6}$  showed little dependence with the substituent and medium. However, the  $\sigma_{\text{C}_2\text{-H}_2} \rightarrow \pi^*_{\text{C}=\text{Y}}$  and  $\sigma_{\text{C}_6\text{H}_6} \rightarrow \pi^*_{\text{C}=\text{Y}}$  interactions are higher for cyclohexanethiones (**2eq**, **4eq** and **6eq**), since this class of compounds exhibits better donor/acceptor character of the electronic orbitals, as previously described. The paradox of showing smaller  ${}^4J_{\text{H}_2,\text{H}_6}$  in spite of stronger electron delocalizations can be explained by the Fermi contact (FC) term (Table 3), which is about 1 Hz smaller in the thiocarbonyl than in the carbonyl compounds. It is worth remembering that the FC contribution varies with the bond length and hybridization of the carbons involved in the coupling. The other terms, namely the spin-dipolar (SD), paramagnetic spin-orbit (PSO) and diamagnetic (DSO), did not change significantly (or even nothing) between carbonyl and thiocarbonyl compounds. It is important to mention that the term FC is strongly influenced by the hybridization of the carbons that participate in the coupling path: interactions  $\pi_{\text{C}=\text{Y}} \rightarrow \sigma^*_{\text{C}-\text{X}}$  and  $\pi_{\text{C}=\text{Y}} \rightarrow \sigma^*_{\text{C}-\text{H}}$  (Table 5) are higher for thiocarbonyl compounds and affect both the hybridization of the C1, C2 and C6 carbons (Table 4) involved in the coupling, as well as the C-C and C-H bond lengths (Table 5). The Fermi contact (FC) term is also the main transmission component of the long-range  ${}^4J_{\text{FH}}$  coupling to *cis*-2-fluorophenol and *cis*-4-bromo-2-fluorophenol, the coupling rather than being given by hydrogen bonds is attributed by FC.<sup>[34]</sup>

Considering the explicit solvation model, the  $\sigma_{\text{C}_2\text{H}_2} \rightarrow \pi^*_{\text{C}_1=\text{Y}}$  and  $\sigma_{\text{C}_6\text{H}_6} \rightarrow \pi^*_{\text{C}_1=\text{Y}}$  values are higher for thiocarbonyls than carbonyls and these interactions destabilize the form C=S. It is also important to keep in mind that thiocarbonyls (C=S) are more polarized than the carbonyls, in aqueous medium. Thus, the tendency is that the group C = O with sp<sup>2</sup> hybridization and a higher “s” character is preferential when compared to C<sup>+</sup>-O<sup>-</sup> the resonance

hybrid (with  $sp^3$  hybridization and a lower “s” character) as well as  $C^+-S^-$  according to Figure 2a. On the other hand, the  $C^+-S^-$  resonance hybrid (Figure 2b) which has  $sp^3$  type hybridization and a lower “s” character is preferential in equilibrium. This feature is due to the fact that the  $C = S$  bond is very unstable since the bond is formed at 2p for carbon and 3p for sulfur. Consequently, the overlapping of the p-orbitals is poor and practically the bond behaves as a dipole ( $C^+-S^-$ ).<sup>[30]</sup> This explains why  $^4J_{H2, H6}$  was lower for thiocarbonyls than for carbonyls, a lower  $s$  character leads to a lower  $^4J_{H2, H6}$  values considering the FC term. However, by comparing the values of the implicit model (PCM) with the explicit ( $H_2O$  molecules), there was a small increase in the  $^4J_{H2, H6}$  values in some cases, once considered an approximation of the solvation layer. The water molecules tend to interact with other solvent molecules and with the solute. In the case of carbonyl group, the water will form hydrogen bonds with  $C = O$  and consequently this form was more stabilized than  $C^+ - O^-$ . The  $C^+-S^-$  resonance hybrid (preferred at equilibrium, as shown in Figure 2b) is stabilized by water from the charge dispersion effect.

In order to shed some more light on the steric and electronic contributions for the  $J$  coupling constant related to the Fermi contact, natural  $J$ -coupling (NJC) calculations were performed. In fact, the natural bonding orbital (NBO) and natural  $J$  coupling (NJC) methods allow the decomposition of the term FC into Lewis contributions and non-Lewis, according to Equation 1:

$$^4J_{H,H}^{FC} = \Delta ^4J_{H,H}^{Lewis} + ^4J_{H,H}^{non-Lewis} \quad (\text{Equation 1})$$

Lewis or localized contributions correspond to steric interactions, whereas non-Lewis contributions are those derived from electron density delocalizations. Within the NBO-NJC, the term non-Lewis is divided into two contributions: those that correspond to the relocation of a donor's electronic density to an accepting orbital centered on a different region of the molecule, so-called delocalized part, and these relocations between orbital centered in the same binding region, called repolarization part, according to equation 2:

$$^4J_{H,H}^{non-Lewis} = \Delta ^4J_{H,H}^{deloc} + ^4J_{H,H}^{repol} \quad (\text{Equation 2})$$

From the NJC results reported in Table 6, for the carbonyl compounds,  $^4J_{ax} \sim ^4J_{eq}$ , and  $J_{Lewis}$  rules the  $J_{FC}$  contribution of the axial form, **1ax**, **3ax** and **6ax**. However, the equatorial form for the carbonyl compounds, **1eq**, **3eq** and **5eq**,  $J_{non-Lewis}$  rules the  $J_{FC}$  contribution. Turning to the thiocarbonyls compounds,  $^4J_{ax} > ^4J_{eq}$ , and  $J_{Lewis}$  governs the  $J_{FC}$  contribution of **2ax**, **4ax**

and **6ax**. However, for **2eq**, **4eq** and **6eq**,  $J_{\text{non-Lewis}}$  rules the  $J_{\text{FC}}$  contribution. The  ${}^4J$  values are larger for the carbonyls than for thiocarbonyls, as shown in Table 6.<sup>[22]</sup>

## 2 CONCLUSIONS

From our theoretical results, both halogen and solvent do not affect significantly the magnitude of the long-range coupling  ${}^4J_{\text{H2,H6}}$ , which is more sensitive to the difference between C=O and C=S. Hyperconjugative interactions  $\sigma_{\text{C2H2}} \rightarrow \pi^*_{\text{C=Y}}$  and  $\sigma_{\text{C6H6}} \rightarrow \pi^*_{\text{C=Y}}$  (Y = O and S) appear to drive the  ${}^4J_{\text{H2,H6}}$  coupling constant. However, the interactions  $\sigma_{\text{C2H2}} \rightarrow \pi^*_{\text{C=S}}$  and  $\sigma_{\text{C6H6}} \rightarrow \pi^*_{\text{C=S}}$  are stronger than the corresponding interactions for the carbonyl compounds, whereas  ${}^4J_{\text{H2,H6}}$  is higher cyclohexanones than in cyclohexanethiones. This apparent contradiction has its origin in the Fermi contact term, which is influenced by the *s* character and bond lengths between atoms involved in the coupling pathway. In addition, the interaction  $\pi_{\text{C=Y}} \rightarrow \sigma^*_{\text{C-X/C-H}}$  affects these parameters and it is lower for carbonyl compounds. Finally, the water molecules described explicitly have established hydrogen bonding with O (= C), or even with halogen (albeit less importantly). Once considered as an approximation of the solvation layer, the water molecules tend to interact more with each other than with the solute, such that the energies of the donor or acceptor orbitals of cyclohexanone and cyclohexanethione are little affected by the influence of the solvent.

## ACKNOWLEDGEMENTS

Authors are thankful to Fundação de Amparo à Pesquisa do Estado de Minas Gerais (FAPEMIG), Conselho Nacional de Desenvolvimento Científico e Tecnológico (CNPq), and Coordenação de Aperfeiçoamento de Pessoal de Nível Superior (CAPES), for the financial support of this research, as well as by the studentships (to F.M.P.R.) and fellowship (to M.P.F. and T.C.R).

## Conflict of interest

The authors declare no competing financial interest.

## References

- [1] A. Rauk, *Orbital interaction theory of organic chemistry*, Wiley, New York, **2001**.
- [2] J.V. Coelho, M.P. de Freitas, T.C. Ramalho, *Struct. Chem.* **2008**, *19*, 671.
- [3] T.R. Doi, F. Yoshinaga, C.F. Tormena, R. Rittner, R.J. Abraham, *Spectrochim. Acta A* **2005**, *61*, 2221.
- [4] R.J. Abraham, A.D. Jones, M.A. Warne, R. Rittner, C.F. Tormena, *J. Chem. Soc. Perkin Trans. 2* **1996**, *6*, 533.
- [5] C.F. Tormena, M.P. Freitas, R. Rittner, R.J. Abraham, *J. Phys. Chem. A* **2004**, *8*, 5161.
- [6] O. Eisenstein, N.T. Anh, Y. Jean, A. Devaquet, J. Cantacuzene, L. Salem, *Tetrahedron* **1974**, *30*, 1717.
- [7] F. Yoshinaga, C.F. Tormena, M.P. Freitas, R. Rittner, R.J. Abraham. *J. Chem. Soc., Perkin Trans. 2* **2002**, *9*, 1494.
- [8] M.P. Freitas, C.F. Tormena, J.C. Garcia, R. Rittner, R.J. Abraham, E.A. Basso, F.P. Santos, J.C. Cedran, *Journal Phys. Org. Chem.* **2003**, *16*, 833.
- [9] J.V. Coelho, M.P. Freitas, C.F. Tormena, R. Rittner. *Magn. Reson. Chem.* **2009**, *47*, 348.
- [10] A. Bagno, G. Saielli, *WIREs Comput. Mol. Sci.* **2015**, *5*, 228.
- [11] N. Grimblat, A.M. Sarotti, *Chem. Eur. J.* **2016**, *22*, 12246.
- [12] B.T. Pereira, E.F. Silva, M.A. Gonçalves, D.T. Mancini, T.C. Ramalho. *J. Chem.* **2017**, *2017*, 01.
- [13] S. Allenmark, B. Bomgren, H. Borén, P. Lagerström, *Anal. Biochem.* **1984**, *136*, 293.
- [14] J.B. Lino, E.P. Rocha, T.C. Ramalho, *J. Phys. Chem. A* **2017**, *121*, 4486.
- [15] C. Møller, M.S. Plesset, *Phys. Rev.* **1934**, *46*, 618,.
- [16] R.A. Kendall, T.H. Dunning JR, R.J. Harrison, *J. Chem. Phys.* **1992**, *96*, 6806.
- [17] D.E. Woon, T.H. Dunning JR. *J. Chem. Phys.* **1993**, *98*, 1358.
- [18] K.A. Peterson, D.E. Woon, T.H. Dunning JR. *J. Chem. Phys.* **1994**, *100*, 7410.
- [19] M.J. Frisch, G.W. Trucks, H.B. Schlegel, G.E. Scuseria, M.A. Robb, J.R. Cheeseman, G. Scalmani, V. Barone, B. Mennucci, G.A. Petersson, H. Nakatsuji, M. Caricato, X. Li, H.P. Hratchian, A.F. Izmaylov, J. Bloino, G. Zheng, J.L. Sonnenberg, M. Hada, M. Ehara, K. Toyota, R. Fukuda, J. Hasegawa, M. Ishida, T. Nakajima, Y. Honda, O. Kitao, H. Nakai, T. Vreven, J.A. Montgomery Jr, J.E. Peralta, F. Ogliaro, M. Bearpark, J.J. Heyd, E. Brothers, K.N. Kudin, V.N. Staroverov, T. Keith, R. Kobayashi, J. Normand, K. Raghavachari, A. Rendell, J.C. Burant, S.S. Iyengar, J. Tomasi, M. Cossi, N. Rega, J.M. Millam, M. Klene, J.E. Knox, J.B. Cross, V. Bakken, C. Adamo, J. Jaramillo, R.

Gomperts, R.E. Stratmann, O. Yazyev, A.J. Austin, R. Cammi, C. Pomelli, J.W. Ochterski, R.L. Martin, K. Morokuma, V.G. Zakrzewski, G.A. Voth, P. Salvador, J.J. Dannenberg, S. Dapprich, A.D. Daniels, O. Farkas, J.B. Foresman, J.V. Ortiz, J. Cioslowski and D.J. Fox, Gaussian 09, Revision D.01, Gaussian Inc., Wallingford, CT, **2013**.

- [20] E.R. Davidson, *Chem. Phys. Lett.* **1996**, *260*, 514.
- [21] P.J. Stephens, F.J. Devlin, C.F.N. Chabalowski, M.J. Frisch, *J. Phys. Chem.* **1994**, *98*, 11623.
- [22] S.J. Wilkens, W.M. Westler, J.L. Markley, F. Weinhold, *J. Am. Chem. Soc.* **2001**, *123*, 12026.
- [23] J. Tomasi, B. Mennucci, R. Cammi, *Chem. Rev.* **2005**, *105*, 2999.
- [24] G. Tevelde, F.M. Bickelhaupt, E.J. Baerends, C.F. Guerra, S.J.A. Van Gisbergen, J.G. Snijders, T. Ziegler, *J. Comp. Chem.*, **2001**, *22*, 931.
- [25] D.T. Mancini, E.F. Souza, M.S. Caetano, T.C. Ramalho, *Magn. Reson. Chem.* **2014**, *52*, 129.
- [26] G. Casella, A. Bagno, S. Komorovsky, M. Repisky, G. Saielli, *Chem. Eur. J.* **2015**, *21*, 18834.
- [27] M. Karplus, *J. Chem Phys.* **1959**, *30*, 11.
- [28] M. Karplus, *J. Chem Phys.* **1960**, *64*, 1793.
- [29] M. Karplus, Vicinal proton coupling in nuclear magnetic resonance. *J. Am. Chem. Soc.* **1963**, *85*, 2870.
- [30] M.P. Freitas, T.C. Ramalho, *Princípios de estrutura eletrônica e orbitais em química orgânica*, UFLA, Lavras, **2013**.
- [31] A.A. de Castro, I.G. Prandi, K. Kuca, T.C. Ramalho. *Cienc. Agrotec.* **2017**, *41*, 471.
- [32] M. P. Freitas, Ph.D. Thesis, University of Campinas, Campinas, 2003.
- [33] Y.Y. Rusakov, L.B. Krivdin, *Russ. Chem. Soc.* **2013**, *82*, 99.
- [34] R.A. Cormanich, M.A. Moreira, Freitas, M.P., T.C. Ramalho, C. Anconi, R. Rittner, R. H. Contreras, C.F. Tormena, *Mag. Res. Chem.* **2011**, *49*, 763.
- [35] T.L.C. Martins, T.C. Ramalho, J.D. Figueroa-Villar, A.F.C. Flores, C.M.P. Pereira, *Mag. Res. Chem.* **2003**, *41*, 983.

## TABLES

**TABLE 1** Calculated values for long-range coupling constants (Hz) for 2-halo-cyclohexanones and 2-halo-cyclohexanethiones. The data for the gas phase, DMSO, H<sub>2</sub>O (implicit solvent model-PCM) and explicit H<sub>2</sub>O are separated by bars.

<b>Compound</b>	<b><math>^4J_{\text{H2,H6}}</math></b>
<b>1ax</b>	0.5/0.5/0.5/0.7
<b>1eq</b>	1.7/1.7/1.7/1.7
<b>2ax</b>	0.3/0.3/0.3/0.4
<b>2eq</b>	0.8/0.8/0.8/0.7
<b>3ax</b>	0.7/0.7/0.7/1.0
<b>3eq</b>	1.9/1.9/1.9/2.1
<b>4ax</b>	0.4/0.7/0.7/0.4
<b>4eq</b>	0.8/1.0/1.0/1.2
<b>5ax</b>	0.9/0.9/0.9/0.9
<b>5eq</b>	2.2/2.2/2.2/2.4
<b>6ax</b>	0.6/0.6/0.6/0.4
<b>6eq</b>	0.9/1.2/1.2/0.5

**TABLE 2** Hyperconjugative interactions (kcal mol<sup>-1</sup>) relevant for <sup>4</sup>J<sub>H<sub>2</sub>,H<sub>6</sub></sub>. Theoretical data (B3LYP/aug-cc-pVTZ) for the gas phase, DMSO, H<sub>2</sub>O (implicit solvent model-PCM) and H<sub>2</sub>O (explicit solvent) are separated by bars.

<b>Compound</b>	$\sigma_{\text{C2H2}} \rightarrow \pi^*_{\text{C1=Y}}$	$\sigma_{\text{C6H6}} \rightarrow \pi^*_{\text{C1=Y}}$	$n_{\text{Y}} \rightarrow \sigma^*_{\text{C1-C2}}$	$n_{\text{Y}} \rightarrow \sigma^*_{\text{C1-C6}}$
<b>1ax</b>	–	–	21.8/21.8/21.8/21.0	20.6/20.6/20.6/19.5
<b>1eq</b>	5.7/5.6/5.6/5.8	6.1/6.1/6.1/6.7	23.2/22.2/23.2/25.0	20.3/19.8/20.3/20.7
<b>2ax</b>	–	–	14.7/14.7/14.7/8.5	16.0/16.0/16.0/7.3
<b>2eq</b>	6.7/6.7/6.7/7.5	6.9/6.8/6.9/8.3	17.0/17.0/17.0/19.2	14.8/14.8/14.8/17.1
<b>3ax</b>	–	–/–/–/0.7	21.6/21.6/21.6/21.4	18.7/20.5/20.4/18.9
<b>3eq</b>	5.2/5.1/5.2/4.3	5.9/5.9/5.9/5.6	23.5/23.5/23.5/24.0	20.6/20.6/20.6/20.4
<b>4ax</b>	–	–/–/–/0.7	15.1/15.0/15.0/18.6	16.2/16.3/16.2/17.6
<b>4eq</b>	5.6/6.0/6.0/5.8	5.8/6.5/6.5/6.9	18.4/17.7/17.6/19.8	15.6/15.2/15.2/17.7
<b>5ax</b>	–	–	21.4/21.4/21.4/21.8	20.5/20.5/18.7/20.1
<b>5eq</b>	5.2/5.2/5.2/5.0	5.9/5.9/5.9/5.8	23.2/23.2/23.2/23.1	20.7/20.7/20.7/20.5
<b>6ax</b>	–	–	15.1/15.1/15.1/17.9	13.2/13.3/16.1/18.7
<b>6eq</b>	5.9/5.9/5.9/5.7	6.3/6.3/6.3/6.5	17.6/17.6/17.6/20.4	15.3/15.3/15.3/18.0

**TABLE 3** FC, DSO, PSO and SD contributions for  ${}^4J_{\text{H}_2,\text{H}_6}$  (in Hz).

<b>Compound</b>	<b>FC</b>	<b>DSO</b>	<b>PSO</b>	<b>SD</b>
<b>1ax</b>	1.0/1.0/1.0/1.2	-1.7/-1.1/-1.7/-0.3	1.2/1.2/1.2/1.1	0.0/0.0/0.0/0.0
<b>1eq</b>	1.2/1.2/1.2/1.0	1.7/1.7/1.7/-1.2	-1.2/-1.2/-1.2/-1.7	0.1/0.1/0.1/0.1
<b>2ax</b>	0.8/0.9/0.9/1.0	-1.7/-1.7/-1.7/2.4	1.1/1.1/1.1/-1.7	0.0/0.0/0.0/0.1
<b>2eq</b>	0.1/0.1/0.1/-0.1	2.0/2.0/2.0/2.4	-1.4/-1.4/-1.4/-1.7	0.1/0.1/0.1/0.1
<b>3ax</b>	1.2/1.2/1.2/1.4	-1.7/-1.7/-1.7/-1.5	1.2/1.2/1.2/1.0	0.0/0.0/0.0/0.0
<b>3eq</b>	1.2/1.2/1.2/1.3	1.8/1.8/1.8/2.6	-1.2/-1.2/-1.2/-1.9	0.1/0.1/0.1/0.1
<b>4ax</b>	0.9/0.9/0.9/1.0	-1.6/-1.6/-1.6/-1.4	1.1/1.1/1.1/0.9	0.0/0.0/0.0/0.0
<b>4eq</b>	0.1/0.1/0.2/0.3	2.2/2.2/2.2/2.3	-1.4/-1.4/-1.4/-1.5	0.1/0.1/0.1/0.0
<b>5ax</b>	1.2/1.2/1.3/1.2	-1.5/-1.5/-1.5/-1.4	1.2/1.2/1.2/1.0	0.0/0.0/0.0/0.0
<b>5eq</b>	1.2/1.2/1.2/1.3	2.1/2.1/2.1/2.8	-1.2/-1.2/-1.2/-1.8	0.1/0.1/0.1/0.0
<b>6ax</b>	1.0/1.0/1.0/0.8	-1.5/-1.6/-1.4/2.7	1.1/1.2/1.0/-1.6	0.0/0.0/0.0/0.0
<b>6eq</b>	0.2/0.2/0.2/0.4	2.5/2.5/2.5/2.7	-1.4/-1.4/-1.4/-1.6	0.1/0.1/0.1/0.1

**TABLE 4** % *s* character for the C1, C2 and C6 atoms in gas phase, DMSO, H<sub>2</sub>O (implicit solvent model-PCM) and H<sub>2</sub>O (explicit solvent) are separated by semicolons.

<b>Compound</b>	<b>%<i>s</i><sub>C1-C2</sub></b>	<b>%<i>s</i><sub>C1-C6</sub></b>	<b>%<i>s</i><sub>C2-H2</sub></b>	<b>%<i>s</i><sub>C6-H6</sub></b>
<b>1ax</b>	26.9/26.9/26.9/26.7	35.8/35.8/35.8/35.4	25.3/25.3/25.3/25.1	24.1/24.1/24.1/26.0
<b>1eq</b>	27.2/27.2/27.2/26.5	35.5/35.5/35.5/35.1	23.7/23.7/23.7/22.1	23.9/22.2/22.2/22.8
<b>2ax</b>	31.3/31.3/31.3/29.0	34.8/34.6/34.6/34.2	24.4/24.5/24.5/24.4	21.3/21.7/27.7/25.5
<b>2eq</b>	31.6/31.6/31.6/28.8	28.2/28.2/28.2/35.0	22.7/22.7/22.7/20.9	21.5/21.5/21.5/22.1
<b>3ax</b>	32.7/32.7/32.7/32.9	22.3/22.3/22.3/25.8	25.3/25.3/25.3/26.9	23.8/23.8/23.8/22.0
<b>3eq</b>	32.9/32.9/32.9/32.7	25.9/25.9/25.9/25.6	23.6/23.6/23.6/24.5	22.3/22.3/22.3/21.4
<b>4ax</b>	32.3/32.3/32.3/31.9	28.6/28.6/28.6/27.7	24.6/24.6/24.6/27.7	23.0/23.0/23.0/21.1
<b>4eq</b>	32.5/32.5/32.5/31.6	28.6/28.4/28.4/28.3	22.5/22.9/22.9/22.2	21.4/21.6/21.6/19.3
<b>5ax</b>	33.1/32.7/33.0/32.9	26.1/26.0/26.1/25.6	25.5/25.3/25.5/25.9	23.7/23.7/23.7/23.6
<b>5eq</b>	32.9/32.9/32.9/33.1	26.0/26.0/26.0/25.6	23.9/23.9/23.6/25.7	22.3/22.3/22.3/22.6
<b>6ax</b>	32.7/32.7/32.3/31.7	28.6/28.6/28.6/27.6	24.9/24.9/24.6/24.4	21.5/21.5/21.5/23.0
<b>6eq</b>	32.5/32.8/32.5/31.8	28.6/28.4/28.4/27.5	22.5/23.2/22.9/25.1	21.4/21.6/21.6/21.9

**TABLE 5** Hyperconjugative interactions involving the  $\pi_{C=Y}$  orbital (kcal mol<sup>-1</sup>), gas phase, DMSO, H<sub>2</sub>O (implicit solvent model-PCM) and H<sub>2</sub>O (explicit solvent) are separated by semicolons and C-C and C-H (Å) bond distances, in the gas phase and explicit solvent (H<sub>2</sub>O) are separated by semicolons.

<b>Compound</b>	$\pi_{C=Y} \rightarrow \sigma^*_{C-X}$	$\pi_{C=Y} \rightarrow \sigma^*_{C-H2}$	$\pi_{C=Y} \rightarrow \sigma^*_{C-H6}$	<b>C1-C2</b>	<b>C1-C6</b>	<b>C2-H2</b>	<b>C6-H6</b>
<b>1ax</b>	2.8/2.8/2.8/2.4	–	–	1.528/1.522	1.508/1.511	1.099/1.110	1.099/1.063
<b>1eq</b>	–	1.5/1.5/1.5/1.6	1.6/1.6/1.6/1.5	1.524/1.533	1.513/1.510	1.104/1.140	1.104/1.100
<b>2ax</b>	4.8/4.8/4.8/1.6	–	–	1.518/1.515	1.499/1.505	1.094/1.116	1.099/1.059
<b>2eq</b>	–	2.6/2.6/2.6/2.7	2.7/2.7/2.7/2.4	1.511/1.529	1.509/1.505	1.105/1.145	1.106/1.111
<b>3ax</b>	5.8/5.8/5.8/2.3	–	–	1.529/1.538	1.511/1.518	1.097/1.130	1.099/1.125
<b>3eq</b>	–	1.6/1.6/1.6/-	1.5/1.5/1.5/-	1.529/1.534	1.516/1.453	1.102/1.095	1.105/1.129
<b>4ax</b>	5.8/5.8/5.8/3.8	-/-/-/0.7	–	1.515/1.531	1.506/1.507	1.097/1.142	1.099/1.137
<b>4eq</b>	–	2.8/2.8/2.8/2.3	2.9/2.9/2.9/2.9	1.520/1.532	1.516/1.520	1.104/1.106	1.099/1.123
<b>5ax</b>	3.5/3.5/3.5/3.1	–	–	1.529/1.527	1.511/1.512	1.098/1.098	1.099/1.148
<b>5eq</b>	–	1.6/1.6/1.6/1.3	1.6/1.6/1.6/1.6	1.528/1.528	1.517/1.516	1.102/1.102	1.105/1.100
<b>6ax</b>	6.3/6.3/6.3/2.1	–	–	1.512/1.527	1.507/1.512	1.097/1.098	1.099/1.100
<b>6eq</b>	–	2.9/2.6/2.6/2.3	2.9/2.6/2.6/2.7	1.519/1.528	1.517/1.516	1.104/1.102	1.107/1.105

**TABLE 6** NJC calculations (in Hz) for  ${}^4J_{\text{H2,H6}}$ . Theoretical data (B3LYP/aug-cc-pVTZ) for the gas phase.

<b>Compoud</b>	$J_{\text{Lewis}}$	$J_{\text{Repol.}}$	$J_{\text{Deloc.}}$	$J_{\text{FC}}$
<b>1ax</b>	0.65	0.07	0.28	1.0
<b>1eq</b>	0.02	0.02	1.16	1.2
<b>2ax</b>	0.53	0.01	0.26	0.8
<b>2eq</b>	-4.99	1.54	3.55	0.1
<b>3ax</b>	0.9	-0.02	0.32	1.2
<b>3eq</b>	0.08	0.01	1.11	1.2
<b>4ax</b>	0.51	0.08	0.31	0.9
<b>4eq</b>	-0.97	0.04	1.03	0.1
<b>5ax</b>	0.96	-0.01	0.67	1.2
<b>5eq</b>	0.09	0.03	1.08	1.2
<b>6ax</b>	0.74	0.07	0.19	1.0
<b>6eq</b>	-0.03	-0.02	0.25	0.2

## FIGURES

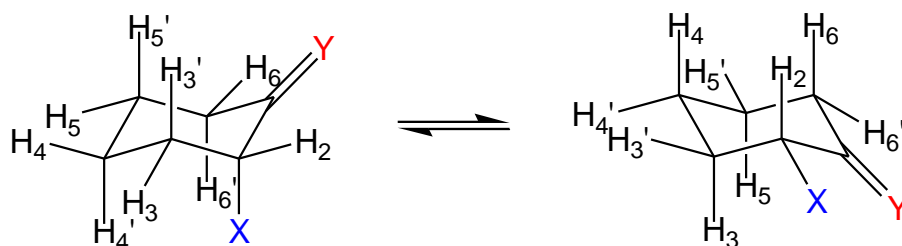


**FIGURE 1** 2-Halo-cyclohexanones and 2-halo-cyclohexanones theoretically studied (1: Y = O, X = F; 2: Y = S, X = F; 3: Y = O, X = Cl; 4: Y = S, X = Cl; 5: Y = O, X = Br; 6: Y = S, X = Br).

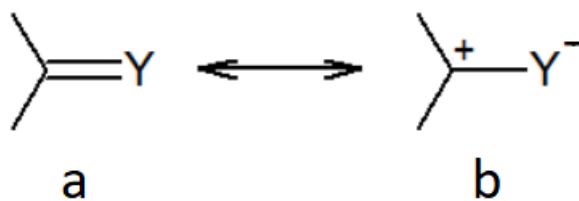


**FIGURE 2** Resonance structure for the carbonyl (Y = O) and thiocarbonyl (Y = S) groups. Structure "b" contributes more for the resonance hybrid in the thiocarbonyl than in the carbonyl group.

## Supporting Information

Probing long-range spin-spin coupling constants in 2-halo-substituted cyclohexanones and cyclohexanethiones: the role of stereoelectronic effects

Fátima M. P. de Rezende, Matheus P. Freitas, Teodorico C. Ramalho\*

*Department of Chemistry, Federal University of Lavras, 37200-000, Lavras, MG, Brazil*

\*Corresponding author: teo@dqi.ufla.br

Page S3. **TABLE S1.** Calculated values for long-range coupling constants (Hz) for 2-halo-cyclohexanones and 2-halo-cyclohexanethiones. The data for the gas phase, DMSO, H<sub>2</sub>O (implicit solvent model-PCM) and explicit H<sub>2</sub>O are separated by stripes

Page S4. **TABLE S2.** Hyperconjugative interactions (kcal mol<sup>-1</sup>) relevant for <sup>4</sup>J<sub>H2,H6</sub>. Theoretical data (B3LYP/aug-cc-pVTZ) for the gas phase, DMSO, H<sub>2</sub>O (implicit solvent model-PCM) and H<sub>2</sub>O (explicit solvent) are separated by stripes

Page S5. **TABLE S3.** X, Y and Z coordinates for **1ax** in the gas

Page S6. **TABLE S4.** X, Y and Z coordinates for **1eq** in the gas

Page S7. **TABLE S5.** X, Y and Z coordinates for **2ax** in the gas

Page S8. **TABLE S6.** X, Y and Z coordinates for **2eq** in the gas

Page S9. **TABLE S7.** X, Y and Z coordinates for **3ax** in the gas

Page S10. **TABLE S8.** X, Y and Z coordinates for **3eq** in the gas

Page S11. **TABLE S9.** X, Y and Z coordinates for **4ax** in the gas

Page S12. **TABLE S10.** X, Y and Z coordinates for **4eq** in the gas

Page S13. **TABLE S11.** X, Y and Z coordinates for **5ax** in the gas

Page S14. **TABLE S12.** X, Y and Z coordinates for **5eq** in the gas

Page S15. **TABLE S13.** X, Y and Z coordinates for **6ax** in the gas

Page S14. **TABLE S14.** X, Y and Z coordinates for **6eq** in the gas

**TABLE S1** Calculated values for long-range coupling constants (Hz) for 2-halo-cyclohexanones and 2-halo-cyclohexanethiones. The data for the gas phase, DMSO, H<sub>2</sub>O (implicit solvent model-PCM) and explicit H<sub>2</sub>O are separated by stripes.

Compound	$^3J_{\text{H2,H3}}$	$^4J_{\text{H2,H4}}$	$^4J_{\text{H2,H4}'}$	$^4J_{\text{H2,H6}'}$	$^4J_{\text{H4,H6}}$
<b>1ax</b>	3.6/3.6/3.6/3.7	-0.2/-0.2/-0.2/-0.2	-0.9/-0.9/-0.9/-0.8	-0.6/-0.6/-0.6/-0.5	0.6/0.6/0.6/0.6
<b>1eq</b>	9.0/9.0/9.0/9.9	0.4/0.4/0.4/0.4	-0.7/-0.7/-0.7/-0.7	-0.6/-0.6/-0.6/-0.4	0.3/0.3/0.3/0.4
<b>2ax</b>	3.9/3.9/3.9/3.6	-0.3/-0.3/-0.3/-0.2	-0.8/-0.8/-0.8/-0.7	-0.7/-0.7/-0.7/-0.6	0.7/0.7/0.7/-0.4
<b>2eq</b>	8.3/8.3/8.3/9.6	0.4/0.4/0.4/0.4	-0.7/-0.7/-0.7/-0.7	-0.6/-0.6/-0.6/-0.6	0.3/0.3/0.3/-0.5
<b>3ax</b>	2.6/2.6/2.6/4.0	0.2/0.2/0.2/1.5	-0.9/-0.9/-0.9/-0.7	-0.7/-0.7/-0.7/-0.2	0.7/0.7/0.7/-0.2
<b>3eq</b>	9.7/9.7/9.7/9.6	-0.5/-0.5/0.5/0.7	-0.5-0.5/-0.5/-0.7	-0.3/-0.3/-0.3/0.2	0.3/0.3/0.3/-0.2
<b>4ax</b>	2.9/0.1/0.1/0.4	0.1/0.3/0.3/2.0	-0.9/-0.9/-0.9/-0.9	-0.7/-0.7/-0.7/-0.7	0.7/0.7/0.7/0.7
<b>4eq</b>	9.1/9.1/9.1/8.3	0.5/0.5/0.5/0.5	-0.5/-0.5/-0.5/-0.5	-0.4/-0.4/-0.4/-0.3	0.4/0.3/0.3/-0.2
<b>5ax</b>	2.8/2.7/2.8/2.9	0.4/0.4/0.4/0.4	-0.9/-0.9/-0.9/-0.9	-0.6/-0.6/-0.6/-0.7	0.8/0.8/0.8/0.8
<b>5eq</b>	10.1/10.1/10.1/9.8	0.7/0.7/0.7/0.9	-0.3/-0.3/-0.3/-0.2	-0.1/-0.1/-0.1/-0.1	0.4/0.4/0.4/0.5
<b>6ax</b>	2.8/3.4/3.4/2.9	0.5/0.5/0.5/0.5	-0.8/-0.8/-0.8/-0.9	-0.7/-0.7/-0.7/-0.8	0.8/0.8/0.8/1.0
<b>6eq</b>	9.4/9.4/9.4/9.3	0.8/0.8/0.8/0.9	-0.3/-0.3/-0.3/-0.2	-0.2/-0.2/-0.2/-0.2	0.4/0.4/0.4/-0.4

**TABLE S2** Hyperconjugative interactions (kcal mol<sup>-1</sup>) relevant for <sup>4</sup>J<sub>H<sub>2</sub>,H<sub>6</sub></sub>. Theoretical data (B3LYP/aug-cc-pVTZ) for the gas phase, DMSO, H<sub>2</sub>O (implicit solvent model-PCM) and H<sub>2</sub>O (explicit solvent) are separated by stripes.

Compound	$\sigma_{\text{C2H2} \rightarrow \sigma^*_{\text{C1C6}}}$	$\sigma_{\text{C6H6} \rightarrow \sigma^*_{\text{C1C2}}}$	$\sigma_{\text{C2H2} \rightarrow \sigma^*_{\text{C3-C4}}}$	$\sigma_{\text{C6H6} \rightarrow \sigma^*_{\text{C4-C5}}}$
<b>1ax</b>	3.4/3.4/3.4/3.4	-/-/3.5	2.7/2.7/2.7/2.6	2.6/2.6/2.6/2.5
<b>1eq</b>	-	3.8/3.6/3.8/ -	-	2.6/2.8/2.6/ -
<b>2ax</b>	4.1/4.1/4.1/2.1	4.7/4.7/4.7/2.2	2.7/2.7/2.7/1.3	2.6/2.6/2.6/1.2
<b>2eq</b>	2.2/ -/-/ -	4.2/4.2/4.2/ -	-	2.6/2.6/2.6/ -
<b>3ax</b>	4.0/4.0/4.0/3.3	-/-/4.5	2.9/2.9/2.9/2.0	2.6/4.4/2.6/2.7
<b>3eq</b>	-	4.1/4.1/4.1/ -	-	-
<b>4ax</b>	4.7/4.7/4.7/4.0	4.9/ -/4.9/5.5	2.9/2.9/2.9/1.9	2.6/2.6/2.6/2.8
<b>4eq</b>	-	4.2/4.3/4.3/ -	-	2.7/2.6/2.6/ -
<b>5ax</b>	4.2/4.2/4.2/4.2	4.4/4.4/4.4/4.5	3.0/3.0/3.0/3.0	2.7/2.7/2.7/2.7
<b>5eq</b>	-	4.1/4.1/4.1/ -	-	-
<b>6ax</b>	4.9/4.9/4.9/-	4.9/4.9/4.9/5.3	3.0/3.0/3.0/2.9	2.6/2.8/2.6/2.7
<b>6eq</b>	-	-	-	2.6/2.6/2.6/-

**TABLE S3** X, Y and Z coordinates for **1ax** in the gas.

Atom	X	Y	Z
C	0.90735300	0.92188700	-0.89085900
C	-0.45971500	1.06134400	-0.22821400
C	-1.08986500	-0.32171700	-0.06747800
C	-0.26271200	-1.29585200	0.73316100
C	1.11398100	-1.43132700	0.03143500
C	1.79705100	-0.06337500	-0.11511700
H	-1.14060000	1.73394300	-0.76838200
H	0.73917500	0.55487800	-1.91980500
H	1.37125700	1.91855700	-0.96717100
H	-0.11105600	-0.89046700	1.74781400
H	-0.78978500	-2.25838300	0.79712400
H	1.74730300	-2.12077900	0.61185100
H	0.96540500	-1.88148100	-0.96638400
H	2.75879300	-0.17704700	-0.64058900
O	-2.13167800	-0.61303700	-0.65972000
F	-0.28231400	1.60567500	1.08016600
H	2.01720000	0.34823500	0.88423900

**TABLE S4** X, Y, Z coordinates for **1eq** in the gas.

Atom	X	Y	Z
C	-0.19208400	-1.45623400	-0.31611000
C	0.80609700	-0.55566100	0.41343300
C	0.51959700	0.90645200	0.09154300
C	-0.89151200	1.33617900	0.42982300
C	-1.89960600	0.41165800	-0.29193600
C	-1.63100200	-1.05930200	0.05437300
H	0.73844200	-0.70246600	1.50538900
H	-0.03576400	-1.34059000	-1.40303400
H	0.01494000	-2.50435500	-0.04963200
H	-1.03423400	1.24155300	1.52136800
H	-1.01790500	2.39101000	0.14583800
H	-2.92365000	0.69808900	-0.00493600
H	-1.81029900	0.55800900	-1.38288900
H	-2.33726100	-1.71259800	-0.48218100
O	1.35294200	1.63532100	-0.44663300
F	2.12293100	-0.88761800	0.03348800
H	-1.79312100	-1.22120600	1.13499000

**TABLE S5** X, Y and Z coordinates for **2ax** in the gas.

Atom	X	Y	Z
C	-0.78156500	0.03405600	0.20679900
C	0.10042400	-1.14716300	-0.14880000
C	1.25098400	-0.67519000	-1.03757500
C	2.02803600	0.47027600	-0.37032400
C	1.09387200	1.62760500	0.00843600
C	-0.05565100	1.13532900	0.92802700
H	1.90289500	-1.53682200	-1.25598100
H	-0.48062000	-1.96282700	-0.60103600
H	2.81335300	0.82673700	-1.05651700
H	1.65123200	2.42340800	0.52862600
H	0.65301400	2.06965800	-0.90309300
H	0.38303000	0.73082300	1.85749500
H	-0.74771400	1.95146800	1.17983300
H	0.81243400	-0.33749300	-1.99357400
S	-2.32643600	0.12858900	-0.33746600
F	0.65404600	-1.66500200	1.06544500
H	2.53233500	0.09316200	0.53531500

**TABLE S6** X, Y and Z coordinates for **2eq** in the gas.

Atom	X	Y	Z
C	-1.68803400	-1.24496300	-0.27619400
C	-0.45364400	-1.43384300	0.63936900
C	0.58315800	-0.39622000	0.28546200
C	0.05860100	1.00985300	0.46264200
C	-1.15632300	1.22168300	-0.44728900
C	-2.24299100	0.17840900	-0.14265400
H	-0.76571800	-1.28630000	1.69033300
H	-0.02446800	-2.44072200	0.53593300
H	-1.38984800	-1.43648900	-1.32228200
H	-2.45349600	-1.99015300	-0.00632500
H	-0.21853400	1.15794000	1.52169900
H	-1.53184600	2.24596600	-0.29521600
H	-0.81787600	1.12812900	-1.49416000
H	-3.09114300	0.32569600	-0.83049300
S	2.06193500	-0.74332300	-0.33091700
F	1.03573600	1.98318900	0.16493500
H	-2.62426900	0.33088400	0.88275700

**TABLE S7** X, Y and Z coordinates for **3ax** in the gas.

Atom	X	Y	Z
C	-1.98674100	-0.43722500	-0.40605800
C	-1.15200600	0.75665500	-0.92762800
C	-0.17461900	1.19057100	0.13987300
C	0.71210100	0.08734200	0.71934800
C	-0.11925700	-1.12432000	1.14865600
C	-1.07649300	-1.58890600	0.04311500
H	-0.58054500	0.43487700	-1.81514800
H	-1.78227700	1.61512600	-1.20091800
H	-2.60763000	-0.10285500	0.44433700
H	-2.67274600	-0.77033100	-1.20097500
H	1.31787500	0.49833700	1.53758400
H	0.55746500	-1.93176800	1.47124800
H	-0.70247800	-0.80871600	2.03404000
H	-1.68460100	-2.42712800	0.41967900
O	-0.11531300	2.33550100	0.59393000
H	-0.49834700	-1.96469800	-0.81834600
Cl	1.90340400	-0.38420900	-0.58392900

**TABLE S8** X, Y and Z coordinates for **3eq** in the gas.

Atom	X	Y	Z
C	2.29618600	-0.00679100	-0.29229700
C	1.53648700	1.12421300	0.43779300
C	0.06261200	1.05668200	0.09114800
C	-0.56230900	-0.29864300	0.42346400
C	0.19527400	-1.41520500	-0.31374500
C	1.68850500	-1.37303600	0.04860900
H	1.64574300	0.98678400	1.52850600
H	1.91465100	2.12005500	0.16443400
H	2.24030300	0.16270800	-1.38214600
H	3.35975100	0.02961000	-0.00816500
H	-0.49875300	-0.45314400	1.51311400
H	-0.25144000	-2.38481700	-0.04444400
H	0.06389400	-1.27161500	-1.40069800
H	2.21397700	-2.17256700	-0.49826600
O	-0.54984700	1.97503900	-0.44986900
H	1.81319300	-1.57703400	1.12712700
Cl	-2.31782800	-0.33903600	0.01350900

**TABLE S9** X, Y and Z coordinates for **4ax** in the gas.

Atom	X	Y	Z
C	0.55466600	-2.03783900	-0.40952000
C	-0.38282800	-1.03324700	-1.12536100
C	-0.88632700	-0.03227600	-0.11946800
C	0.19222500	0.70782400	0.64561700
C	1.16993100	-0.27978400	1.29489100
C	1.70750600	-1.30644900	0.29034600
H	0.19566400	-0.50059500	-1.90128000
H	-1.23067100	-1.54385500	-1.60383000
H	-0.03228400	-2.60901900	0.33207300
H	0.94054600	-2.75589500	-1.15116500
H	-0.25103200	1.39317600	1.37921400
H	1.98297100	0.28635300	1.77742500
H	0.60525000	-0.79770500	2.09253400
H	2.35028700	-2.02884400	0.81929400
O	-2.46866500	0.17140000	0.26924400
H	2.33571700	-0.79822000	-0.46102900
Cl	1.08653800	1.79428400	-0.53236300

**TABLE S10** X, Y and Z coordinates for **4eq** in the gas.

Atom	X	Y	Z
C	2.37247600	0.28314800	-0.23040800
C	1.41519500	1.07301600	0.69434000
C	-0.01229600	0.78427800	0.28693500
C	-0.33082000	-0.69156500	0.43477800
C	0.59588900	-1.49927600	-0.49505800
C	2.06830900	-1.21713100	-0.15933800
H	1.56841100	0.73559200	1.73641300
H	1.60655800	2.15411200	0.63900500
H	2.24678600	0.64512000	-1.26638200
H	3.41307400	0.48676200	0.06966700
H	-0.15769700	-0.98455500	1.48384700
H	0.36285000	-2.56951400	-0.38085100
H	0.37477900	-1.20970200	-1.53750400
H	2.71057400	-1.77354000	-0.86155700
S	-1.00968000	1.91694900	-0.35111700
H	2.29106000	-1.59192200	0.85550500
Cl	-2.05376700	-1.11519800	0.09954300

**TABLE S11** X, Y and Z coordinates for **5ax** in the gas.

Atom	X	Y	Z
C	-2.30455800	-0.67473100	- 0.58215700
C	-1.56884000	0.61406300	-1.01574800
C	-0.80090700	1.18762400	0.15393000
C	0.10666700	0.21639900	0.90452700
C	-0.60487700	-1.09810700	1.23299700
C	-1.32254600	-1.69220300	0.01489700
H	-0.84849200	0.36480400	-1.81402700
H	-2.26099800	1.38156300	-1.39106800
H	-3.07439600	-0.42042200	0.16812400
H	-2.82603500	-1.10168400	-1.45348900
H	0.51964100	0.71324800	1.79224500
H	0.11694500	-1.80714400	1.66881400
H	-1.34881200	-0.86286700	2.01787900
H	-1.86037100	-2.60405600	0.32080900
O	-0.92189800	2.35091700	0.54614700
Br	1.67172100	-0.10859300	-0.26231000
H	-0.58216300	-1.98829000	-0.74829800

**TABLE S12** X, Y and Z coordinates for **5eq** in the gas.

Atom	X	Y	Z
C	2.82454000	-0.12811500	-0.29772300
C	2.14671500	1.05323000	0.43275300
C	0.66911400	1.08751700	0.09324200
C	-0.04186400	-0.22241000	0.42953100
C	0.63361900	-1.39111300	-0.30769000
C	2.12771800	-1.44896000	0.05004900
H	2.25053100	0.91101500	1.52340300
H	2.59078100	2.02041800	0.15545700
H	2.77483000	0.04202700	-1.38781000
H	3.88961500	-0.16259700	-0.01886500
H	0.01066500	-0.37968900	1.51922500
H	0.12472200	-2.32831100	-0.03420400
H	0.50957800	-1.24457800	-1.39516100
H	2.59582100	-2.28439500	-0.49554100
O	0.12265600	2.04957200	-0.44267200
B/r	-1.94651000	-0.14327600	0.00413500
H	2.24100000	-1.65671800	1.12917600

**TABLE S13** X, Y and Z coordinates for **6ax** in the gas.

Atom	X	Y	Z
C	-1.39022700	-1.95272800	-0.57522900
C	-1.29620100	-0.53431900	-1.18877300
C	-1.07821600	0.47141800	-0.08799500
C	0.09918600	0.19483300	0.81925200
C	0.06587900	-1.24106100	1.35685900
C	-0.13516000	-2.27702500	0.24505800
H	-0.43082800	-0.50287200	-1.87501000
H	-2.20333000	-0.27821300	-1.75455700
H	-2.28438600	-2.00599100	0.07162800
H	-1.52592300	-2.68431400	-1.38822200
H	0.15735900	0.93920300	1.62351500
H	0.98396600	-1.43304700	1.93509900
H	-0.78586100	-1.28570200	2.06196700
H	-0.22294100	-3.27932700	0.69509200
S	-2.10011800	1.71739400	0.23407200
Br	1.75925400	0.49645000	-0.23181500
H	0.74837700	-2.29052600	-0.41617700

**TABLE S14** X, Y and Z coordinates for **6eq** in the gas.

Atom	X	Y	Z
C	2.83321300	-0.36304600	-0.21192900
C	2.14919600	0.67243700	0.71026000
C	0.70269600	0.83532600	0.28420000
C	-0.04975500	-0.47687000	0.41826200
C	0.60096100	-1.52268800	-0.50951100
C	2.08739900	-1.70162000	-0.16152800
H	2.18254000	0.30011000	1.75217100
H	2.65726300	1.64658300	0.66667900
H	2.83281600	0.02917200	-1.24473100
H	3.88540000	-0.48920700	0.09289900
H	0.01760700	-0.81623900	1.46635500
H	0.05493800	-2.47443000	-0.41300400
H	0.48631600	-1.17404300	-1.55124700
H	2.54130700	-2.42322000	-0.86145700
S	0.11458200	2.22280900	-0.35643000
Br	-1.96028900	-0.36257500	0.05042700
H	2.17633700	-2.13477500	0.85175500

**ARTIGO 2****The Perlin effect in 2-halocyclohexanones and 2-halocyclohexanothiones**

*Fátima M. P. de Rezende<sup>1</sup>, Matheus P. Freitas<sup>1</sup>, Teodorico C. Ramalho<sup>1,2\*</sup>*

<sup>1</sup>Department of Chemistry, Federal University of Lavras, 37200-000, Lavras, MG, Brazil.

<sup>2</sup>Center for Basic and Applied Research, Faculty of Informatics and Management, University of Hradec Kralove, Rokitanskeho 62, 50003, Czech Republic.

**KEYWORDS:** Perlin effect, one-bond coupling constant, Fermi contact, Lewis-type interactions

**HIGHLIGHTS:**

- The Perlin effect  $^1J_{C-H_{ax}} < ^1J_{C-H_{eq}}$  was observed for all compounds
- Perlin effect is stronger in 2-halocyclohexanothiones than in the respective ketones
- The medium does not affect the Perlin effect

**Normas do Periódico: Computational and Theoretical Chemistry**  
(versão publicada)

**ABSTRACT**

The Perlin effect is an NMR phenomenon observed in six-membered rings and it is referred to as  $^1J_{\text{C-Hax}} < ^1J_{\text{C-Heq}}$ . In the present work, the influence of halogens (F, Cl and Br) at position 2 in cyclohexanones and cyclohexanethiones is theoretically evaluated on the one-bond C2–H2 coupling constants, *i.e.* on the Perlin effect. An important hyperconjugative interaction ( $\pi_{\text{C=Y}} \rightarrow \sigma^*_{\text{C-H}}$ , Y = O and S) operating in the studied systems seems to play a significant role for the observed  $^1J_{\text{C-Hax}} < ^1J_{\text{C-Heq}}$  behavior. In addition, the Lewis contribution ( $J^{\text{Lewis}}$ ) dominates the Fermi Contact term ( $J^{\text{FC}}$ ), which plays the major role for the overall one-bond C–H coupling constant. Compared to the gas phase, this behavior was found to be insensitive to implicit solvents (DMSO and water).

## 1. Introduction

The Perlin effect refers to a smaller spin-spin coupling constant value  $^1J_{\text{C-H}_{\text{ax}}}$  compared to the corresponding  $^1J_{\text{C-H}_{\text{eq}}}$  in six-membered rings, which can be useful to provide information on the stereochemistry and stereoelectronic interactions in alicyclic compounds [1,2]. This phenomenon has been originally attributed to the fact that C-H<sub>ax</sub> bonds are longer than C-H<sub>eq</sub>, due to  $\sigma_{\text{CH}} \rightarrow \sigma^*_{\text{C-H}_{\text{ax}}}$  hyperconjugative interactions in cyclohexane derivatives and to  $n_{\text{O}} \rightarrow \sigma^*_{\text{C-H}_{\text{ax}}}$  interactions in tetrahydropyran derivatives, such as pyranoside sugars. The opposite effect, *i.e.*  $^1J_{\text{C-H}_{\text{ax}}} > ^1J_{\text{C-H}_{\text{eq}}}$ , is observed for some dithianes and it is referred to as the reverse Perlin effect; this effect has been attributed to a better electron transfer  $\sigma_{\text{CS}} \rightarrow \sigma^*_{\text{C-H}_{\text{eq}}}$  compared to  $n_{\text{S}} \rightarrow \sigma^*_{\text{C-H}_{\text{ax}}}$  [3].

Because of the hyperconjugative nature of the Perlin effect, it is often related to the well-known anomeric effect, which is a concept used in carbohydrate chemistry to explain the axial preference of electronegative substituents at the anomeric carbon ( $\alpha$ -anomer) instead of the less sterically hindered equatorial orientation ( $\beta$ -anomer) in a pyranoside ring [3]. The cause and consequence of the Perlin and anomeric effects, respectively, lie in the fact C<sub>2</sub>-H<sub>ax</sub> bond is longer and weaker than C<sub>2</sub>-H<sub>eq</sub> in tetrahydropyran (THP); the longer C<sub>2</sub>-H<sub>ax</sub> bond would be due to a  $n_{\text{O}} \rightarrow \sigma^*_{\text{C-H}_{\text{ax}}}$  interaction, decreasing the electronic occupancy in the corresponding C-H orbital and then disfavoring the coupling transmission. Dipolar effects have also been reported as driving interactions of the Perlin effect and of a related phenomenon observed in organofluorine compounds [4-7]. The carbonyl group effect on the  $^1J_{\text{C2-F}}$  coupling constant in cyclohexanone derivatives has also demonstrated the role of electrostatic interactions on this NMR parameter [8]. Additional arguments based on induced current densities have also appeared recently to explain the Perlin effect [9].

In 1969, Perlin and Casu [1] observed an approximate 10 Hz difference in the  $^1J_{\text{C-H}}$  coupling constants at the anomeric centers of anomeric glycoside pairs. In the case of D-glucose,

the anomer  $\alpha$ , which contains an equatorial hydrogen in C1, exhibited the highest coupling constant value. The C1-H equatorial bond on a pyranose ring is shorter and stronger than the axial C1-H bond. Since the Fermi contact term is the main contribution to the coupling between directly connected cores, it is not surprising that the magnitude of  $^1J_{C-H}$  coupling constants relates inversely with the C-H bond length. However, this behavior has not been profoundly studied in cyclohexanone rings, thus motivating a theoretical analysis of the one-bond coupling constants in 2-haloketones, that is a wide-spread moiety in many compounds of chemical and biological interest [10,11].

In addition, because hyperconjugation possibly plays an important role on the Perlin effect, as well as the  $\pi$  system as electron-donating group in stereoelectronic interactions, the influence of a thiocarbonyl group on the vicinal one-bond C-H coupling constant of halogenated derivatives may be useful to be analyzed. It is well known that the magnitude of a one-bond C-H coupling constant depends upon the chemical environment of the hydrogen atom and, especially, upon its stereochemical relationship to vicinal lone electron pairs. However, a lone electron pair is not essential for the observation of a stereoelectronic effect, since even cyclohexane exhibits different axial and equatorial C-H coupling constants. Thus, it was proposed the name "Perlin Effect" to describe such observations. An analysis of the experimental data regarding the Perlin Effect show that, in cyclohexane and in six-membered rings having one or more heteroatoms of the first row attached to the carbon of interest,  $^1J_{C-H}$  is always larger for an equatorial hydrogen than for an axial hydrogen.

The Perlin Effect has application in the elucidation of the structures of chemical compounds, because it is possible to determine if there is an equatorial hydrogen or axial hydrogen in six-membered rings. In the current paper, we have evaluated the influence of halogen substituents on the magnitude of a one-bond C-H coupling constant. To our knowledge, this is the first application of theoretical studies to evaluate the origin of the Perlin

Effect as well as the halogen influence in gas and condensed phase of 2-halocyclohexanones and 2-halocyclohexanethiones. It is well known that the magnitude of a one-bond C–H coupling constant depends upon the chemical environment of the hydrogen atom and, especially, upon its stereochemical relationship to vicinal lone electron pairs. However, a lone electron pair is not essential for the observation of a stereoelectronic effect, since even cyclohexane exhibits different axial and equatorial C–H coupling constants. Thus, the name "Perlin Effect" to describe such observations was proposed.

An analysis of the experimental data regarding the Perlin Effect show that, in cyclohexane and in six-membered rings having one or more heteroatoms of the first row attached to the carbon of interest,  $^1J_{C-H}$  is always larger for an equatorial hydrogen than for an axial hydrogen. The Perlin Effect has application in the elucidation of the structures of chemical compounds, because it is possible to determine if there is an equatorial hydrogen or axial hydrogen in six-membered rings. Thus, the following compounds of Figure 1 were studied with the aim at further investigating the manifestation and origin of the so-called Perlin. To our knowledge, this is the first application of theoretical studies to evaluate the origin of the Perlin Effect as well as the halogen influence in gas and condensed phase of 2-halocyclohexanones and 2-halocyclohexanethiones.

Thus, the following compounds of Figure 1 were studied with the aim at further investigating the manifestation and origin of the so-called Perlin effect.

## 2. Computational procedure

Compounds of Figure 1 were fully optimized at the  $\omega$ B97XD/6-31g(d,p)[12-13] level, either for the isolated molecule (gas phase) and considering implicit solvents (DMSO and water), according to the polarizable continuum model (PCM) [14], using the Gaussian 09 program [15]. The electron delocalization and Lewis-type energies and interactions were

obtained on the basis of Natural Bond Orbital (NBO) [15] analyses at the same level of theory, as well as the spin-spin coupling constant calculations [16-17]  $J$ -coupling analysis were evaluated through the Natural J-Coupling (NJC) framework [18].

### 3. Results and Discussion

The Perlin effect  ${}^1J_{\text{C2-H2ax}} < {}^1J_{\text{C2-H2eq}}$  was observed for all compounds **1-6**, according to Table 1. Accordingly, the bond distances were all longer for **1ax**, **2ax**, **3ax**, **4ax**, **5ax** and **6ax** (the axial and equatorial conformers in Table 1 were named according to the orientation of the C–H2 bond). This behavior is consistent with a more effective electronic delocalization towards the axial  $\sigma^*_{\text{C-H}}$  orbital, that elongates and weakens the C–Hax bond. The theoretical values of  ${}^1J_{\text{C-H}}$  presented a difference of approximately 7% with respect to the experimental  ${}^1J_{\text{C-H}}$  values [2].

The C–H bond distance ( $d_{\text{C-H}}$ ) in the axial conformers is expected to be lengthened in comparison to the equatorial conformers as result of an important hyperconjugative interaction  $\pi_{\text{C=O}} \rightarrow \sigma^*_{\text{C-H2}}$  (Table 2) [8]. This interaction in thiocarbonyl compounds appears to be, in general, a little more effective than in carbonyl compounds (Table 2), which can be due to a higher acidity of  $\alpha$ -thiocarbonyl hydrogens compared to  $\alpha$ -carbonyl hydrogens. In addition, the  $n_{\text{X}} \rightarrow \sigma^*_{\text{C-H}}$  electron delocalization is also expected to elongate the C–H<sub>ax</sub> bond, and a subtle dependence of this interaction with both X and Y is observed: it is stronger according to  $\text{Br} < \text{Cl} < \text{F}$ , and more effective in thiocarbonyl than in carbonyl compounds in gas phase. According to our findings (Figure 1-4), it has not been observed a precise relationship between the calculated increase in bond length and decrease in  ${}^1J_{\text{CH}}$  for 2-halocyclohexanones and 2-halocyclohexanothiones. It should be kept in mind, however, that the Fermi contact (FC, responsible for the magnitude of  ${}^1J$  coupling constants) in C–H bonds, as well as the bond distance, is strongly influenced by hybridization in the

bond forming carbon. This means, the larger  $s$ -character is proportional to the larger FC term and a shorter C–H bond[19]. For 2-fluorometanol, a linear dependence of  $^1J_{CF}$  with  $d(C-F)$ [20], however an angular dependence of this coupling with the  $d(C-F)$  for carbonyl system have not been evaluated. For these systems, just an angular with hyperconjugatives interactions and dipole moments has been observed[21].

Because the overall  $^1J_{C-H2}$  spin-spin coupling constant results from the contribution of Fermi contact (FC), spin dipolar (SD), paramagnetic spin-orbit (PSO) and diamagnetic spin-orbit (DSO) terms (Equation 1), the reason for these findings can be found in Table 3. While the SD, PSO and DSO terms are nearly insensitive to  $Y$ , the FC contribution is higher in thiocarbonyl than in carbonyl compounds, and this is accompanied as the solvent changes.

$$^1J_{C2-H2} = ^1J_{C2-H2}^{FC} + ^1J_{C2-H2}^{SD} + ^1J_{C2-H2}^{PSO} + ^1J_{C2-H2}^{DSO} \quad (1)$$

The Fermi contact (FC) term, the major responsible for the magnitude of the  $^1J_{C-H}$  coupling constants in **1-6**, is strongly influenced by the hybridization at the bound carbon; the higher its  $s$ -character (Table 4), the higher the FC term[20]. Comparing the halogen series, the  $^1J_{C-H2}$  values are similar for  $X=F$  and  $Cl$  (**1**, **2**, **3** and **4**), but decrease when  $X=Br$  (**5** and **6**) (Table 1); this trend is accompanied by the FC term (Table 3) and, subsequently, by the  $s$ -character at C2 (Table 4). On the other hand, the electronic occupancy (Table 5) is higher for equatorial conformers. To explain this behavior, natural  $J$ -coupling analysis (NJC data in Table 6) was carried out and the FC term was thoroughly evaluated. It is worth keeping in mind that within an atom, only  $s$ -orbitals have non-zero electron density at the nucleus, then, the contact interaction only occurs for  $s$ -electrons. Accordingly, it is expected that a higher  $s$ -character leads to higher FC contributions. However, another interesting aspect to consider regarding the

FC term is the Lewis and non-Lewis contributions to  ${}^1J_{\text{C-H2}}^{\text{FC}}$ . Therefore, the  ${}^1J_{\text{C-H2}}^{\text{FC}}$  was decomposed into these contributions (Equation 2) on the basis of a NJC analysis [18].

$${}^1\Delta J_{\text{C-H2}}^{\text{FC}} = \Delta J_{\text{C-H2}}^{\text{Lewis}} + \Delta J_{\text{C-H2}}^{\text{non-Lewis}} \quad (2)$$

The Lewis part reflects the character of the orbital according to a Lewis-based scheme (*i.e.* considering the bond, lone pair, or core orbital), while the non-Lewis part is related to all delocalization effects not described in the Lewis scheme. In other words, Lewis or localized contributions correspond to steric interactions, whereas non-Lewis interactions are those derived from electron density delocalizations. Within the NBO-NJC framework, the term non-Lewis is divided into two contributions: those that correspond to the reallocation of a donor's electron density to an accepting orbital centered on a different region of the molecule, the so-called delocalized part. In addition, there are also reallocations around the orbital centered in the same region of connection, called repolarization part, according to Equation 3 [18].

$${}^1\Delta J_{\text{C-H2}}^{\text{non-Lewis}} = \Delta J_{\text{C-H2}}^{\text{deloc}} + \Delta J_{\text{C-H2}}^{\text{repol}} \quad (3)$$

Moreover,  $\Delta J_{\text{C-H2}}^{\text{Lewis}}$  and  $\Delta J_{\text{C-H2}}^{\text{non-Lewis}}$  can be decomposed into individual contributions of different NBO's, occupied and unoccupied, according to Equations 4 [18] and 5 [18].

$$\Delta J_{\text{HH}}^{\text{Lewis}} = \sum_i^{\text{Occ}} \Delta_{i\text{Lewis}} \quad (4)$$

$$\Delta J_{\text{HH}}^{\text{non-Lewis}} = \sum_i^{\text{Occ}} \sum_j^{\text{Unocc}} \Delta_{ij}^{\text{non-Lewis}} \quad (5)$$

According to Table 6, the main component for the magnitude of  ${}^1J^{\text{FC}}_{\text{C2-H2}}$  corresponds to the Lewis term  ${}^1J^{\text{Lewis}}_{\text{C-H2}}$ , while the Perlin effect (translated to  ${}^1J^{\text{FC}}_{\text{C2-H2ax}} < {}^1J^{\text{FC}}_{\text{C2-H2eq}}$ ) can also be described by the delocalization term  ${}^1J^{\text{Deloc}}_{\text{C2-H2}}$ , especially for Cl and Br derivatives, repolarization plays some important role only for compound **1**. It is well known that electron delocalization can play a critical role for the transport of nuclear spin information, especially for higher-order Spin-Spin Coupling Constant (SSCC) [22]. Thus, the  $\Delta {}^1J^{\text{Lewis}}_{\text{C2-H2}}$  and  $\Delta {}^1J^{\text{Deloc}}_{\text{C2-H2}}$  values give insight on the X and Y effects to the Perlin effect. Regarding X, the Lewis contribution to the overall FC term decreases on going from F to Br (for **5**,  ${}^1J^{\text{Lewis}}_{\text{C2-H2ax}}$  is higher than  ${}^1J^{\text{Lewis}}_{\text{C2-H2eq}}$ ), while the delocalization contribution increases in this order. The interplay of interactions governing the behavior of the  ${}^1J_{\text{C-F}}$  SSCC, in particular the role of the Lewis term, is in agreement with earlier studies pointing out that steric and dipolar interactions describe the angular dependence of  ${}^1J_{\text{C-H}}$  and  ${}^1J_{\text{C-F}}$  SSCC [4-8]. Regarding Y in the C=Y bond, the Perlin effect is slightly stronger in thiocarbonyl than in carbonyl compounds, and this behavior is particularly reflected by the Lewis term in the fluorinated derivatives, and by the delocalization term in the other halogen derivatives. There was no significant difference in the data for the gas phase and solution (implicit DMSO and H<sub>2</sub>O). It is important to notice that the use of this solvation model implies to neglect thermal effects, as well as specific interactions between solvent and solute. It is also worth mentioning that for flexible systems, these parameters should be considered for the purpose of a more appropriate description of the thermal and solvation effects [23-27].

#### 4. Conclusions

The medium does not affect the Perlin effect ( ${}^1J_{\text{C-Hax}} < {}^1J_{\text{C-Heq}}$ ), which was an effect observed for the whole set of 2-halocyclohexanones and 2-halocyclohexanethiones studied. The behavior in the  ${}^1J_{\text{C-H2}}$  SSCC is described by the Fermi contact term, and this is ruled by

Lewis and delocalization contributions. The latter is particularly relevant to describe the Perlin effect in Cl and Br derivatives, while the former contributes to the Perlin effect according to  $\text{Br} < \text{Cl} < \text{F}$ . In general, the Perlin effect is stronger in 2-halocyclohexanethiones than in the respective ketones. However, it is practically insensitive to the halogen, *i.e.* the orientation of the C-X bond does not affect  $\Delta^1J_{\text{C-H(ax-eq)}}$ , but the nature of X influences the magnitude of this SSCC, that is, the smaller  $^1J_{\text{C-H}}$  values are observed as larger and less electronegative is the halogen.

### **Acknowledgements**

This study was financed in part by the Coordenação de Aperfeiçoamento de Pessoal de Nível Superior – Brasil (CAPES) - Finance Code 001. The authors wish to thank the financial support the Conselho Nacional de Desenvolvimento Científico e Tecnológico – Brasil (CNPq) and the Fundação de Amparo à Pesquisa do Estado de Minas Gerais – Brasil (FAPEMIG). This work was also supported by excellence project FIM and UHHK.

### AUTHOR INFORMATION

#### **Corresponding Author**

\*Corresponding author: [teo@dqi.ufla.br](mailto:teo@dqi.ufla.br)

**Notes:** The authors declare no competing financial interest.

#### **Author Contributions**

The manuscript was written through contributions of all authors. All authors have given approval to the final version of the manuscript.

## References

- [1] A.S. Perlin, B. Casu, Carbon-13 and proton magnetic resonance spectra of D-glucose-13C, *Tetrahedron Lett.* 10 (1969) 2921–2924. [https://doi.org/10.1016/S0040-4039\(01\)88308-8](https://doi.org/10.1016/S0040-4039(01)88308-8).
- [2] S. Wolfe, B.M. Pinto, V. Varma, R.Y. Leung, The Perlin effect: bond lengths, bond strengths, and the origins of stereoelectronic effects upon one-bond C–H coupling constants, *Can.J. Chem.* 68 (1990) 1051–1062. <https://doi.org/10.1139/v90-164>.
- [3] E. Juaristi, G. Cuevas, Manifestations of stereoelectronic interactions in  $^1J_{C-H}$  one-bond coupling constants, *Accounts Chem. Res.* 40 (2007) 961–970. <https://doi.org/10.1021/ar6000186>.
- [4] G. Cuevas, K. Martínez-Mayorga, M.D.C. Fernández-Alonso, J. Jiménez-Barbero, C.L. Perrin, E. Juaristi, N. López-Mora, The origin of one-bond C–H coupling constants in OCH fragments: not primarily  $n_O \rightarrow$  delocalization, *Angew. Chem.-Int. Edit.* 44 (2005) 2360–2364. <https://doi.org/10.1002/anie.200461583>.
- [5] M.P. Freitas, M. Bühl, D. O'hagan, 1, 2-Difluoroethane: the angular dependence on  $^1J_{CF}$  coupling constants is independent of hyperconjugation, *Chem. Commun.* 48 (2012) 2433–2435. <https://doi.org/10.1039/C2CC17180E>.
- [6] M.P. Freitas, M. Bühl, D. O'hagan, R.A. Cormanich, C.F. Tormena, Stereoelectronic interactions and the one-bond C–F coupling constant in sevoflurane, *J. Phys. Chem. A* 116 (2012) 1677–1682. <https://doi.org/10.1021/jp211949m>.
- [7] J.M. Silla, M.P. Freitas, R.A. Cormanich, R. Rittner, The reverse fluorine perlin-like effect and related stereoelectronic interactions, *J. Org. Chem.* 79 (2014) 6385–6388. <https://doi.org/10.1021/jo501025a>.
- [8] J.M. Silla, M.P. Freitas, The mutual effect of a carbonyl polar bond and an endocyclic oxygen on the  $^1J_{C-F}$  coupling constant of fluorinated six-membered rings, *Magn. Reson. Chem.* 55 (2017) 10791083. <https://doi.org/10.1002/mrc.4632>.
- [9] J.G. Hernández-Lima, J.E. Barquera-Lozada, G. Cuevas, F. Cortés-Guzmán, The role of induced current density in stereoelectronic effects: Perlin effect, *J. Comput. Chem.* 36 (2015) 1573–1578. <https://doi.org/10.1002/jcc.23965>.
- [10] G. Pattison, Conformational preferences of  $\alpha$ -fluoroketones may influence their reactivity, *Beilstein J. Org. Chem.* 13 (2017) 2915–2921. <https://doi.org/10.3762/bjoc.13.284>.

- [11] D.B. Rubinov, I.L. Rubinova, A.A. Akhrem, Chemistry of 2-Acylcycloalkane-1, 3-diones, *Chem.Rev.* 99 (1999) 1047–1066. <https://doi.org/10.1021/cr9600621>.
- [12] J. Chai, M. Head-Gordon, Long-range corrected hybrid density functionals with damped atom–atom dispersion corrections, *Phys. Chem. Chem. Phys.* 10(2008) 6615–6620. <https://doi.org/10.1039/B810189B>
- [13] M.J. Frisch, J.A. Pople, J.S. Binkley, Self-consistent molecular orbital methods 25: Supplementary functions for Gaussian basis sets, *J.Chem.Phys.* 80 (1984) 3265–3269.
- [14] J. Tomasi, B. Mennucci, R. Cammi, Quantum mechanical continuum solvation models, *Chem.Rev.* 105 (2005) 2999–3094. <https://doi.org/10.1021/cr9904009>.
- [15] M.J. Frisch, G.W. Trucks, H.B. Schlegel, G.E. Scuseria, M.A. Robb, J.R. Cheeseman, G. Scalmani, V. Barone, B. Mennucci, G.A. Petersson, H. Nakatsuji, M. Caricato, X. Li, H.P. Hratchian, A.F. Izmaylov, J. Bloino, G. Zheng, J.L. Sonnenberg, M. Hada, M. Ehara, K. Toyota, R. Fukuda, J. Hasegawa, M. Ishida, T. Nakajima, Y. Honda, O. Kitao, H. Nakai, T. Vreven, J.A. Montgomery, J.E. Peralta Jr., F. Ogliaro, M. Bearpark, J.J. Heyd, E. Brothers, K.N. Kudin, V.N. Staroverov, R. Kobayashi, J. Normand, K. Raghavachari, A. Rendell, J.C. Burant, S.S. Iyengar, J. Tomasi, M. Cossi, N. Rega, J.M. Millam, M. Klene, J.E. Knox, J.B. Cross, V. Bakken, C. Adamo, J. Jaramillo, R. Gomperts, R.E. Stratmann, O. Yazyev, A.J. Austin, R. Cammi, C. Pomelli, J.W. Ochterski, R.L. Martin, K. Morokuma, V.G. Zakrzewski, G.A. Voth, P. Salvador, J.J. Dannenberg, S. Dapprich, A.D. Daniels, O. Farkas, J.B. Foresman, J.V. Ortiz, J. Cioslowski, D.J. Fox, *Gaussian 09, Revision D.01*, Gaussian Inc., Wallingford, 2009.
- [16] A.D. Becke, A new mixing of Hartree–Fock and local density-functional theories, *J. Chem. Phys.* 98 (1993) 1372–1377. <https://doi.org/10.1063/1.464304>.
- [17] D.P. Chong, *Recent Advances in Density Functional Methods, Part I*, first ed., World Scientific Publ. Co, Singapore, 1996.
- [18] S.J. Wilkens, W.M. Westler, J.L. Markley, F. Weinhold, Natural J-coupling analysis: Interpretation of scalar J-couplings in terms of Natural Bond Orbitals, *J. Am.Chem. Soc.* 123 (2001) 12026–12036. <https://doi.org/10.1021/ja016284k>.
- [19] Y.Y. Rusakov, L.B. Krivdin, Modern quantum chemical methods for calculating spin–spin coupling constants: theoretical basis and structural applications in chemistry, *Russ.Chem. Rev.* 82 (2013) 99–130. <https://doi.org/10.1070/RC2013v082n02ABEH004350>.

- [20] J.M.Silla, M. P. Freitas. Polar and stereoelectronic effects on the structural and spectroscopic properties of halomethanols. *Comput. Theor.Chem.* 1037 (2014) 49-52. <https://doi.org/10.1016/j.comptc.2014.04.007>.
- [21] M.P Freitas, M. Buhl. Density functional study of the one-bond CF coupling constant in  $\alpha$ -fluorocarbonyl and  $\alpha$ -fluorosulfonyl compounds. *J. Fluor. Chem.* 140 (2012) 82-87. <https://doi.org/10.1016/j.jfluchem.2012.05.007>.
- [22] D. Cremer, J. Gräfenstein, Calculation and analysis of NMR spin–spin coupling constants, *Phys.Chem. Chem.Phys.* 9 (2007) 2791–2816. <https://doi.org/10.1039/B700737J>.
- [23] T.C. Ramalho, M. Bühl, Probing NMR parameters, structure and dynamics of 5-nitroimidazole derivatives: Density functional study of prototypical radiosensitizers, *Magn. Reson. Chem.*43 (2005) 139–146. <https://doi.org/10.1002/mrc.1514>.
- [24] M.S. Caetano, T.C. Ramalho, D.F Botrel, E.F. Da Cunha, W.C. De Mello, Understanding the inactivation process of organophosphorus herbicides: A DFT study of glyphosate metallic complexes with Zn<sup>2+</sup>, Ca<sup>2+</sup>, Mg<sup>2+</sup>, Cu<sup>2+</sup>, Co<sup>3+</sup>, Fe<sup>3+</sup>, Cr<sup>3+</sup>, and Al<sup>3+</sup>, *Int. J. Quantum Chem.* 112 (2012) 2752–2762. <https://doi.org/10.1002/qua.23222>.
- [25] T. C. Ramalho, C.A. Taft. Thermal and solvent effects on the NMR and UV parameters of some bioreductive drugs, *J. Chem. Phys.* 123 (2005) 054319. <https://doi-org.ez26.periodicos.capes.gov.br/10.1063/1.1996577>.
- [26] A. da Silva Gonçalves , T.C.C França, M .S Caetano, T. C. Ramalho, T. C. (2014). Reactivation steps by 2-PAM of tabun-inhibited human acetylcholinesterase: reducing the computational cost in hybrid QM/MM methods. *J. Biomol. Struct. Dyn.* 32 (2014) 301-307. <https://doi.org/10.1080/07391102.2013.765361>.
- [27] K. Kuca, K., O. Soukup , P. Maresova, J. Korabecny, E. Nepovimova, B.Klimova, Honeg J., B., T.C. Ramalho, T.C.C. França. Current approaches against Alzheimer's disease in clinical trials. *J. Braz. Chem. Soc.* 27 (2016) 641-649. <http://dx.doi.org/10.5935/0103-5053.201600>.

**Table 1** Calculated relative conformational energies ( $E_{\text{rel}}$  in kcal mol<sup>-1</sup>, obtained at the  $\omega$ B97X-D/6-31G(d,p) level),  $^1J_{\text{C-H2}}$  (in Hz, obtained at the  $\omega$ B97X-D/6-311+G(d,p) level), molecular dipole moments ( $\mu$ , in Debye), and C–X bond lengths (in Å), for compounds **1-6**.

Cp	Gas				DMSO				H <sub>2</sub> O			
	$E_{\text{rel}}$	$^1J_{\text{C-H2}}$	$\mu$	$d_{\text{C-H}}$	$E_{\text{rel}}$	$^1J_{\text{C-H2}}$	$\mu$	$d_{\text{C-H}}$	$E_{\text{rel}}$	$^1J_{\text{C-H2}}$	$\mu$	$d_{\text{C-H}}$
<b>1ax</b>	0.5	135.5	4.3	1.10108	0.0	135.2	5.4	1.10152	0.0	135.5	5.4	1.10152
<b>1eq</b>	0.0	149.9	2.8	1.09307	1.3	145.9	3.5	1.09568	1.4	145.9	3.5	1.09567
<b>2ax</b>	0.58	137.7	4.3	1.10128	0.0	137.6	5.8	1.10215	0.0	137.6	5.9	1.10215
<b>2eq</b>	0.0	149.4	2.8	1.09230	1.4	150.9	3.7	1.09434	1.4	149.4	3.7	1.09433
<b>3ax</b>	0.75	135.1	4.6	1.09602	0.0	135.1	6.0	1.09802	0.0	135.1	6.0	1.09800
<b>3eq</b>	0.0	145.6	3.2	1.09265	1.21	145.5	4.1	1.09266	1.24	145.6	4.1	1.09265
<b>4ax</b>	2.3	137.9	4.4	1.08963	0.5	137.9	6.1	1.09832	0.4	137.9	6.1	1.09830
<b>4eq</b>	0.0	149.8	3.1	1.08863	0.0	149.8	4.1	1.09096	0.0	149.8	4.1	1.09097
<b>5ax</b>	2.5	129.3	4.4	1.09498	0.7	134.6	5.8	1.09733	0.6	134.7	5.8	1.09388
<b>5eq</b>	0.0	142.8	4.0	1.08864	0.0	145.1	4.0	1.09200	0.0	145.1	4.0	1.08835
<b>6ax</b>	4.0	133.2	4.2	1.09488	2.3	139.7	5.9	1.09762	2.3	137.9	5.9	1.09379
<b>6eq</b>	0.0	146.9	3.1	1.08774	0.0	145.1	4.1	1.09040	0.0	149.8	4.2	1.08740

**Table 2** NBO electron delocalization energies (in kcal mol<sup>-1</sup>) obtained for **1-6** in the gas phase/DMSO/H<sub>2</sub>O.

<b>Compound</b>	$n_x \rightarrow \sigma^*_{C-H}$	$\pi_{C=Y} \rightarrow \sigma^*_{C-H}$
<b>1ax</b>	8.3/6.7/6.7	1.8/1.7/1.7
<b>1eq</b>	7.6/4.7/6.2	-
<b>2ax</b>	9.2/7.1/7.1	2.1/2.1/2.1
<b>2eq</b>	2.2/2.1/2.1	-
<b>3ax</b>	4.2/3.6/3.6	2.0/1.9/1.9
<b>3eq</b>	3.4/2.8/2.8	-
<b>4ax</b>	4.2/3.6/2.8	2.0/1.9/1.9
<b>4eq</b>	3.1/2.8/2.8	-
<b>5ax</b>	3.9/2.9/2.9	2.1/1.6/1.6
<b>5eq</b>	2.4/2.3/2.3	-
<b>6ax</b>	4.2/2.6/2.7	1.5/1.9/1.9
<b>6eq</b>	2.2/2.1/2.1	-

**Table 3** The Ramsey terms (Fermi contact, spin dipolar, paramagnetic spin-orbit, and diamagnetic spin-orbit) for  $^1J_{C-H}$  (in Hz) in **1-6** (gas phase/DMSO/water).

<b>Compound</b>	<b>FC</b>	<b>SD</b>	<b>PSO</b>	<b>DSO</b>
<b>1ax</b>	134.4/134.3/134.4	0.16/0.16/0.16	-0.57/-0.57/-0.57	1.54/1.31/1.54
<b>1eq</b>	149.1/145.2/145.2	0.25/0.25/0.25	-0.79/-0.79/-0.79	1.29/1.29/1.29
<b>2ax</b>	136.7/136.7/136.7	0.16/0.15/0.15	-0.55/-0.55/-0.55	1.38/1.38/1.38
<b>2eq</b>	148.6/150.0/148.6	0.27/0.23/0.27	-0.76/-0.65/-0.76	1.33/1.35/1.33
<b>3ax</b>	133.8/133.8/133.8	0.27/0.27/0.27	-0.27/-0.27/-0.27	1.29/1.29/1.29
<b>3eq</b>	144.5/144.5/144.5	0.37/0.37/0.37	-0.55/-0.55/-0.55	1.24/1.23/1.24
<b>4ax</b>	136.6/136.6/136.6	0.28/0.28/0.28	-0.25/-0.25/-0.25	1.32/1.32/1.32
<b>4eq</b>	148.7/148.7/148.7	0.41/0.41/0.41	-0.52/-0.52/-0.52	1.25/1.25/1.25
<b>5ax</b>	127.5/133.1/133.2	0.26/0.32/0.32	-0.17/-0.37/-0.38	1.67/1.57/1.56
<b>5eq</b>	141.2/143.9/143.9	0.34/0.40/0.40	-0.50/-0.66/-0.66	1.73/1.50/1.50
<b>6ax</b>	131.4/138.1/136.3	0.27/0.32/0.34	-0.17/-0.31/-0.34	1.69/1.59/1.59
<b>6eq</b>	148.1/143.9/148.4	0.40/0.47/0.46	-0.52/-0.67/-0.63	1.61/1.40/1.53

**Table 4** % *s*-character for the C2, H<sub>ax</sub> and H<sub>eq</sub> atoms in gas phase/DMSO/H<sub>2</sub>O).

Compound	% <i>s</i> C <sub>2</sub>	% <i>s</i> H <sub>ax</sub>	% <i>s</i> H <sub>eq</sub>
<b>1ax</b>	24.7/25.1/25.1	99.9/99.9/99.9	-
<b>1eq</b>	27.0/27.0/27.0	-	99.9/99.0/99.0
<b>2ax</b>	24.2/24.6/24.6	99.9/99.9/99.9	-
<b>2eq</b>	26.9/27.0/27.0	-	99.9/99.0/99.0
<b>3ax</b>	24.5/25.2/25.2	99.9/99.0/99.0	-
<b>3eq</b>	26.6/26.9/26.9	-	99.9/99.0/99.0
<b>4ax</b>	24.1/25.0/25.0	99.9/99.0/99.0	-
<b>4eq</b>	26.7/27.0/27.0	-	99.9/99.0/99.0
<b>5ax</b>	25.2/25.3/25.3	99.9/99.9/99.9	-
<b>5eq</b>	27.1/27.3/27.3	-	99.9/99.9/99.9
<b>6ax</b>	25.0/27.4/27.4	99.9/99.9/99.9	-
<b>6eq</b>	27.2/27.4/27.4	-	99.9/99.9/99.9

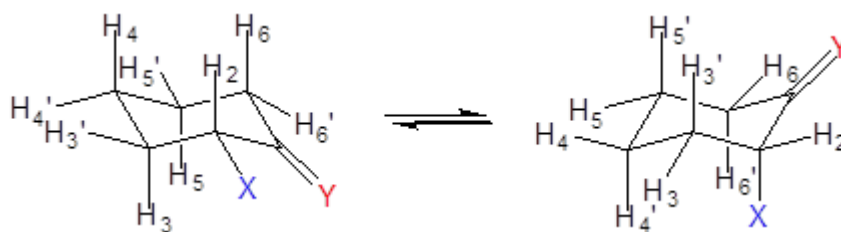
**Table 5** Electronic occupancies at  $\sigma_{\text{C-H}_2}$  in gas phase/DMSO/H<sub>2</sub>O.

<b>Compound</b>	<b>C-H<sub>2</sub> Occupancy</b>
<b>1ax</b>	1.96638/1.96641/1.96638
<b>1eq</b>	1.98251/1.98251/1.98251
<b>2ax</b>	1.95931/1.95937/1.95931
<b>2eq</b>	1.98286/1.98286/1.98286
<b>3ax</b>	1.96868/1.96873/1.96868
<b>3eq</b>	1.98239/1.98239/1.98239
<b>4ax</b>	1.96542/1.96542/1.96550
<b>4eq</b>	1.98318/1.98318/1.98318
<b>5ax</b>	1.97083/1.96784/1.96784
<b>5eq</b>	1.98279/1.98279/1.98278
<b>6ax</b>	1.96568/1.96436/1.96432
<b>6eq</b>	1.98358/1.98364/1.98369

**Table 6** NJC results (in Hz) for  $^1J_{C-H}$ . Theoretical data obtained at the  $\omega$ B97XD/6-31g (d,p) level for the gas phase molecules.

<b>Compound</b>	$^1J_{C-H}^{Lewis}$	$^1J_{C-H}^{Repol}$	$^1J_{C-H}^{Deloc}$	$^1J_{C-H}^{FC}$
<b>1ax</b>	183.0	-5.84	-42.8	134.4
<b>1eq</b>	190.8	-3.69	-41.6	145.2
<b>2ax</b>	187.4	-5.39	-45.3	136.7
<b>2eq</b>	196.0	-4.30	-43.1	148.6
<b>3ax</b>	180.2	-4.59	-41.8	133.8
<b>3eq</b>	185.2	-4.22	-36.5	144.5
<b>4ax</b>	184.9	-4.14	-44.2	136.6
<b>4eq</b>	190.5	-4.57	-37.2	148.7
<b>5ax</b>	174.6	-3.90	-43.2	127.2
<b>5eq</b>	170.7	-3.93	-35.2	141.2
<b>6ax</b>	169.7	3.90	-43.2	130.4
<b>6eq</b>	185.6	-4.26	-35.9	148.0

**Figure 1** 2-Halocyclohexanones [**1** (X = F), **3**(X = Cl) and **5** (X = Br), and Y = O] and 2-halocyclohexanothiones [**2** (X = F), **4**(X = Cl) and **6** (X = Br), and Y = S] theoretically studied.



### 3 CONCLUSÃO GERAL

No Artigo 1, tanto o halogênio quanto o solvente não afetaram significativamente a magnitude do acoplamento de longo alcance  ${}^4J_{\text{H}2, \text{H}6}$ , que é mais sensível à diferença entre  $\text{C} = \text{O}$  e  $\text{C} = \text{S}$ . Interações hiperconjugativas  $\sigma_{\text{C}2\text{H}2} \rightarrow \pi^*_{\text{C}=\text{Y}}$  e  $\sigma_{\text{C}6\text{H}6} \rightarrow \pi^*_{\text{C}=\text{Y}}$  ( $\text{Y} = \text{O}$  e  $\text{S}$ ) parecem conduzir a constante de acoplamento  ${}^4J_{\text{H}2, \text{H}6}$ . No entanto, as interações  $\sigma_{\text{C}2\text{H}2} \rightarrow \pi^*_{\text{C}=\text{S}}$  e  $\sigma_{\text{C}6\text{H}6} \rightarrow \pi^*_{\text{C}=\text{S}}$  são mais fortes que as interações correspondentes para os compostos carbonílicos, enquanto que  ${}^4J_{\text{H}2, \text{H}6}$  são maiores para as ciclohexanonas do que para as ciclohexanotionas. Essa aparente contradição tem sua origem no termo de contato Fermi, que é influenciado pelo caráter s e comprimentos de ligação entre os átomos envolvidos na via de acoplamento. Finalmente, as moléculas de água descritas explicitamente estabeleceram ligação de hidrogênio com  $\text{O} (= \text{C})$ , ou mesmo com halogênio (embora menos importante). Uma vez consideradas como uma aproximação da camada de solvatação, as moléculas de água tendem a interagir mais umas com as outras do que com o soluto. Para o Artigo 2, o meio não afetou o efeito Perlin ( ${}^1J_{\text{C-Hax}} < {}^1J_{\text{C-Heq}}$ ), que foi um efeito observado para todo o conjunto de 2-halociclohexanonas e 2-halociclohexanotionas estudadas. O comportamento nos SSCCs  ${}^1J_{\text{C-H}2}$  é descrito pelo termo de contato Fermi, e isso é governado por contribuições de Lewis e de deslocalização. Em geral, o efeito Perlin é mais forte em 2-halociclohexanotionas do que nas respectivas cetonas. No entanto, é praticamente insensível ao halogênio.